



SUSITNA-WATANA HYDRO

Clean, reliable energy for the next 100 years.

ALASKA ENERGY AUTHORITY

AEA11-022

13-1407-REP-030714

Appendix D

Storm Precipitation Analysis System (SPAS) Program Description

INTRODUCTION

The Storm Precipitation Analysis System (SPAS) is grounded on years of scientific research with a demonstrated reliability in hundreds of post-storm precipitation analyses. It has evolved into a trusted hydrometeorological tool that provides accurate precipitation data at a high spatial and temporal resolution for use in a variety of sensitive hydrologic applications (Faulkner et al. 2004, Tomlinson et al. 2003-2012). Applied Weather Associates, LLC and METSTAT, Inc. initially developed SPAS in 2002 for use in producing Depth-Area-Duration values for Probable Maximum Precipitation (PMP) analyses. SPAS utilizes precipitation gauge data, “basemaps” and radar data (when available) to produce gridded precipitation at time intervals as short as 5-minutes, at spatial scales as fine as 1 km² and in a variety of customizable formats. To date (February 2014) SPAS has been used to analyze over 330 storm centers across all types of terrain, among highly varied meteorological settings and some occurring over 100-years ago.

SPAS output has many applications including, but not limited to: hydrologic model calibration/validation, flood event reconstruction, storm water runoff analysis, forensic cases and PMP studies. Detailed SPAS-computed precipitation data allow hydrologists to accurately model runoff from basins, particularly when the precipitation is unevenly distributed over the drainage basin or when rain gauge data are limited or not available. The increased spatial and temporal accuracy of precipitation estimates has eliminated the need for commonly made assumptions about precipitation characteristics (such as uniform precipitation over a watershed), thereby greatly improving the precision and reliability of hydrologic analyses.

To instill consistency in SPAS analyses, many of the core methods have remained consistent from the beginning. However, SPAS is constantly evolving and improving through new scientific advancements and as new data and improvements are incorporated. This write-up describes the current inter-workings of SPAS, but the reader should realize SPAS can be customized on a case-by-case basis to account for special circumstances; these adaptations are documented and included in the deliverables. The overarching goal of SPAS is to combine the strengths of rain gauge data and radar data (when available) to provide sound, reliable and accurate spatial precipitation data.

Hourly precipitation observations are generally limited to a small number of locations, with many basins lacking observational precipitation data entirely. However, Next Generation Radar (NEXRAD) data provide valuable spatial and temporal information over data-sparse basins, which have historically lacked reliability for determining precipitation rates and reliable quantitative precipitation estimates (QPE). The improved reliability in SPAS is made possible by hourly calibration of the NEXRAD radar-precipitation relationship, combined with local hourly bias adjustments to force consistency between the final result and “ground truth” precipitation measurements. If NEXRAD radar data are available (generally for storm events since the mid-1990’s), precipitation accumulation at temporal scales as frequent as 5-minutes can be analyzed. If

no NEXRAD data are available, then precipitation data are analyzed in hourly increments. A summary of the general SPAS processes are shown in flow chart in Figure D.1.

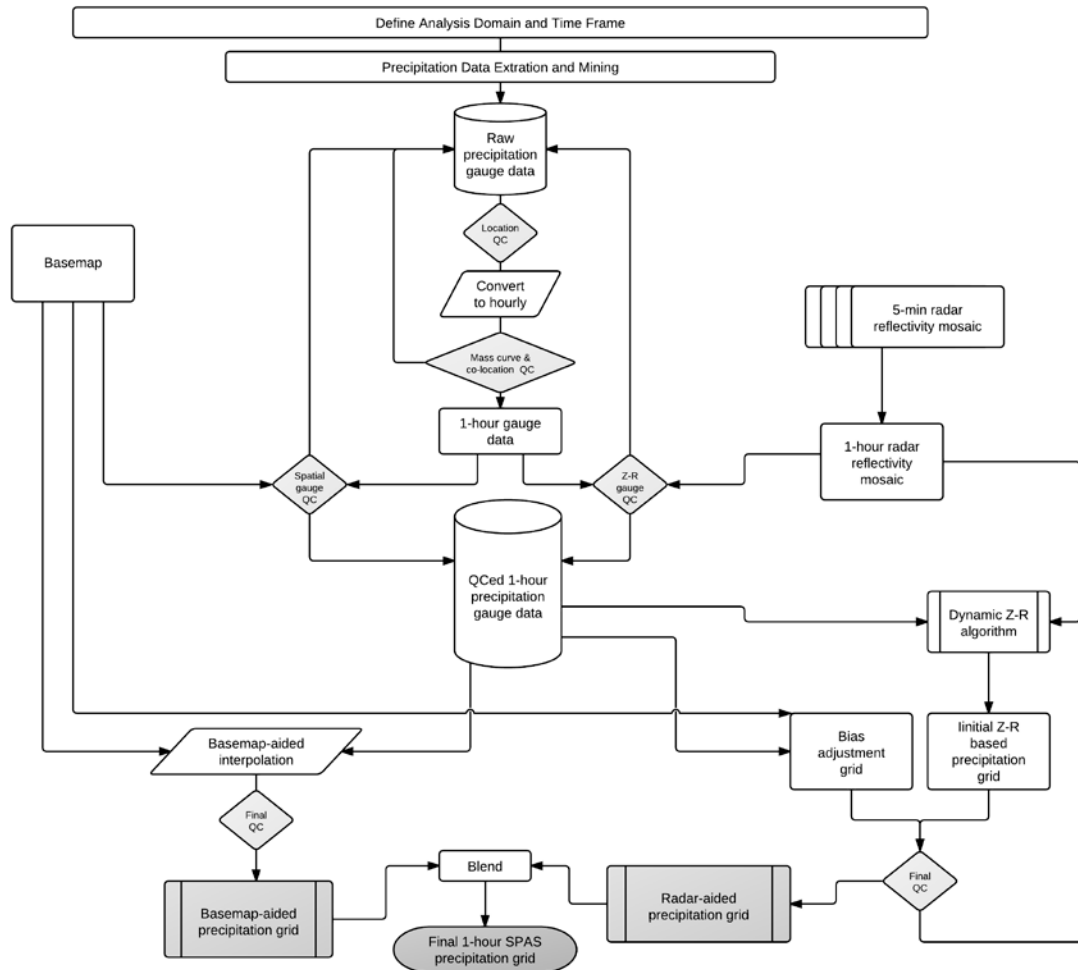


Figure D.1. SPAS flow chart.

SETUP

Prior to a SPAS analysis, careful definition of the storm analysis domain and time frame to be analyzed is established. Several considerations are made to ensure the domain (longitude-latitude box) and time frame are sufficient for the given application.

SPAS Analysis Domain

For PMP applications it is important to establish an analysis domain that completely encompasses a storm center, meanwhile hydrologic modeling applications are more concerned about a specific basin, watershed or catchment. If radar data are available, then it is also important to establish an

area large enough to encompass enough stations (minimum of ~30) to adequately derive reliable radar-precipitation intensity relationships (discussed later). The domain is defined by evaluating existing documentation on the storm as well as plotting and evaluating initial precipitation gauge data on a map. The analysis domain is defined to include as many hourly recording gauges as possible given their importance in timing. The domain must include enough of a buffer to accurately model the nested domain of interest. The domain is defined as a longitude-latitude (upper left and lower right corner) rectangular region.

SPAS Analysis Time Frame

Ideally, the analysis time frame, also referred to as the Storm Precipitation Period (SPP), will extend from a dry period through the target wet period then back into another dry period. This is to ensure that total storm precipitation amounts can be confidently associated with the storm in question and not contaminated by adjacent wet periods. If this is not possible, a reasonable time period is selected that is bounded by relatively lighter precipitation. The time frame of the hourly data must be sufficient to capture the full range of daily gauge observational periods for the daily observations to be disaggregated into estimated incremental hourly values (discussed later). For example, if a daily gauge takes observations at 8:00 AM, then the hourly data must be available from 8:00 AM the day prior. Given the configuration of SPAS, the minimum SPP is 72 hours and aligns midnight to midnight.

The core precipitation period (CPP) is a sub-set of the SPP and represents the time period with the most precipitation and the greatest number of reporting gauges. The CPP represents the time period of interest and where our confidence in the results is highest.

DATA

The foundation of a SPAS analysis is the “ground truth” precipitation measurements. In fact, the level of effort involved in “data mining” and quality control represent over half of the total level of effort needed to conduct a complete storm analysis. SPAS operates with three primary data sets: precipitation gauge data, a “basemap” and, if available, radar data. Table D.1 conveys the variety of precipitation gauges usable by SPAS. For each gauge, the following elements are gathered, entered and archived into SPAS database:

- Station ID
- Station name
- Station type (H=hourly, D=Daily, S=Supplemental, etc.)
- Longitude in decimal degrees
- Latitude in decimal degrees
- Elevation in feet above MSL
- Observed precipitation

- Observation times
- Source
- If unofficial, the measurement equipment and/or method is also noted.

Based on the SPP and analysis domain, hourly and daily precipitation gauge data are extracted from our in-house database as well as the Meteorological Assimilation Data Ingest System (MADIS). Our in-house database contains data dating back to the late 1800s, while the MADIS system (described below) contains archived data back to 2002.

Hourly Precipitation Data

Our hourly precipitation database is largely comprised of data from NCDC TD-3240, but also precipitation data from other mesonets and meteorological networks (e.g. ALERT, Flood Control Districts, etc.) that we have collected and archived as part of previous studies. Meanwhile, MADIS provides data from a large number of networks across the U.S., including NOAA’s HADS (Hydrometeorological Automated Data System), numerous mesonets, the Citizen Weather Observers Program (CWOP), departments of transportation, etc. (see http://madis.noaa.gov/mesonet_providers.html for a list of providers). Although our automatic data extraction is fast, cost-effective and efficient, it never captures all of the available precipitation data for a storm event. For this reason, a thorough “data mining” effort is undertaken to acquire all available data from sources such as U.S. Geological Survey (USGS), Remote Automated Weather Stations (RAWS), Community Collaborative Rain, Hail & Snow Network (CoCoRaHS), National Atmospheric Deposition Program (NADP), Clean Air Status and Trends Network (CASTNET), local observer networks, Climate Reference Network (CRN), Global Summary of the Day (GSD) and Soil Climate Analysis Network (SCAN). Unofficial hourly precipitation are gathered to give guidance on either timing or magnitude in areas otherwise void of precipitation data. The WeatherUnderground and MesoWest, two of the largest weather databases on the Internet, contain a good deal of official data, but also includes data from unofficial gauges.

Table D.1 Different precipitation gauge types used by SPAS.

Precipitation Gauge Type	Description
Hourly	Hourly gauges with complete, or nearly complete, incremental hourly precipitation data.
Hourly estimated	Hourly gauges with some estimated hourly values, but otherwise reliable.
Hourly pseudo	Hourly gauges with reliable temporal precipitation data, but the magnitude is questionable in relation to co-located daily or supplemental gauge.
Daily	Daily gauge with complete data and known observation times.
Daily estimated	Daily gauges with some or all estimated data.
Supplemental	Gauges with unknown or irregular observation times, but reliable total storm precipitation data. (E.g. public reports, storms reports, “Bucket surveys”, etc.)
Supplemental estimated	Gauges with estimated total storm precipitation values based on other information (e.g. newspaper articles, stream flow discharge, inferences from nearby gauges, pre-existing total storm isohyetal maps, etc.)

Daily Precipitation Data

Our daily database is largely based on NCDC's TD-3206 (pre-1948) and TD-3200 (1948 through present) as well as SNOTEL data from NRCS. Since the late 1990s, the CoCoRaHS network of more than 15,000 observers in the U.S. has become a very important daily precipitation source. Other daily data are gathered from similar, but smaller gauge networks, for instance the High Spatial Density Precipitation Network in Minnesota.

As part of the daily data extraction process, the time of observation accompanies each measured precipitation value. Accurate observation times are necessary for SPAS to disaggregate the daily precipitation into estimated incremental values (discussed later). Knowing the observation time also allows SPAS to maintain precipitation amounts within given time bounds, thereby retaining known precipitation intensities. Given the importance of observation times, efforts are taken to insure the observation times are accurate. Hardcopy reports of "Climatological Data," scanned observational forms (available on-line from the NCDC) and/or gauge metadata forms have proven to be valuable and accurate resources for validating observation times. Furthermore, erroneous observation times are identified in the mass-curve quality-control procedure (discussed later) and can be corrected at that point in the process.

Supplemental Precipitation Gauge Data

For gauges with unknown or irregular observation times, the gauge is considered a "supplemental" gauge. A supplemental gauge can either be added to the storm database with a storm total and the associated SPP as the temporal bounds or as a gauge with the known, but irregular observation times and associated precipitation amounts. For instance, if all that is known is 3 inches fell between 0800-0900, then that information can be entered. Gauges or reports with nothing more than a storm total are often abundant, but to use them, it is important the precipitation is only from the storm period in question. Therefore, it is ideal to have the analysis time frame bounded by dry periods.

Perhaps the most important source of data, if available, is from "bucket surveys," which provide comprehensive lists of precipitation measurements collected during a post-storm field exercise. Although some bucket survey amounts are not from conventional precipitation gauges, they provide important information, especially in areas lacking data. Particularly for PMP-storm analysis applications, it is customary to accept extreme, but valid non-standard precipitation values (such as bottles and other open containers that catch rainfall) in order to capture the highest precipitation values.

Basemap

“Basemaps” are independent grids of spatially distributed weather or climate variables that are used to govern the spatial patterns of the hourly precipitation. The basemap also governs the spatial resolution of the final SPAS grids, unless radar data are available/used to govern the spatial resolution. Note that a base map is not required as the hourly precipitation patterns can be based on station characteristics and an inverse distance weighting technique (discussed later). Basemaps in complex terrain are often based on the PRISM mean monthly precipitation (Figure D.2a) or Hydrometeorological Design Studies Center precipitation frequency grids (Figure D.2b) given they resolve orographic enhancement areas and micro-climates at a spatial resolution of 30-seconds (about 800 m). Basemaps of this nature in flat terrain are not as effective given the small terrain forced precipitation gradients. Therefore, basemaps for SPAS analyses in flat terrain are often developed from pre-existing (hand-drawn) isohyetal patterns (Figure D.2c), composite radar imagery or a blend of both.

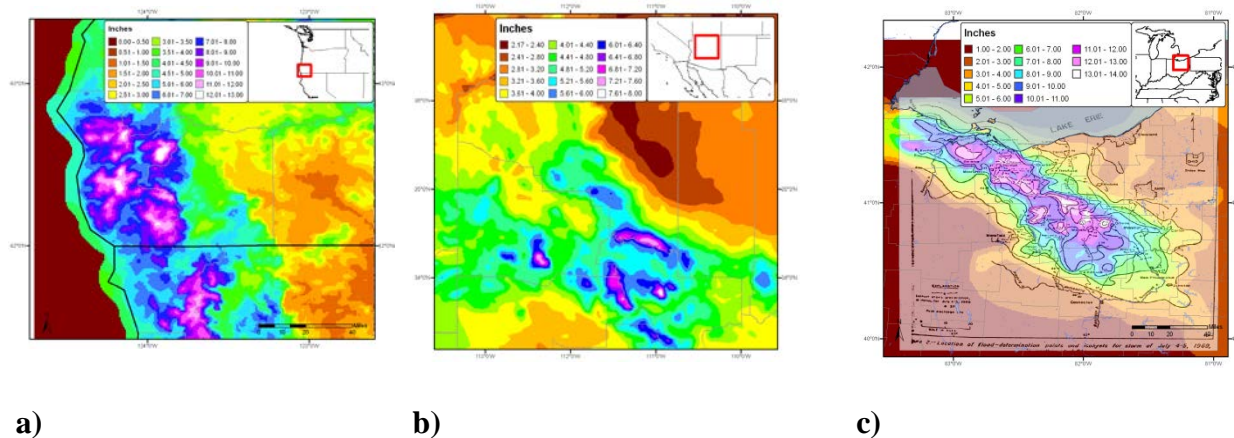


Figure D.2 Sample SPAS “basemaps:” (a) A pre-existing (USGS) isohyetal pattern across flat terrain (SPAS #1209), (b) PRISM mean monthly (October) precipitation (SPAS #1192) and (c) A 100-year 24-hour precipitation grid from NOAA Atlas 14 (SPAS #1138).

Radar Data

For storms occurring since approximately the mid-1990s, weather radar data are available to supplement the SPAS analysis. A fundamental requirement for high quality radar-estimated precipitation is a high quality radar mosaic, which is a seamless collection of concurrent weather radar data from individual radar sites, however in some cases a single radar is sufficient (i.e. for a small area size storm event such as a thunderstorm). Weather radar data have been in use by meteorologists since the 1960s to estimate precipitation depths, but it was not until the early 1990s that new, more accurate NEXRAD Doppler radar (WSR88D) was placed into service across the United States. Currently, efforts are underway to convert the WSR88D radars to dual polarization (DualPol) radar. Today, NEXRAD radar coverage of the contiguous United States is comprised of 159 operational sites and there are 30 in Canada. Each U.S. radar covers an approximate 285 mile

(460 km) radial extent and while Canadian radars have approximately 256 km (138 nautical miles) radial extent over which their radar can detect precipitation. (see Figure E.3) The primary vendor of NEXRAD weather radar data for SPAS is Weather Decision Technologies, Inc. (WDT), who accesses, mosaics, archives and quality-controls NEXRAD radar data from NOAA and Environment Canada. SPAS utilizes Level II NEXRAD radar reflectivity data in units of dBZ, available every 5-minutes in the U.S. and 10-minutes in Canada.

NEXRAD Coverage Below 10,000 Feet AGL

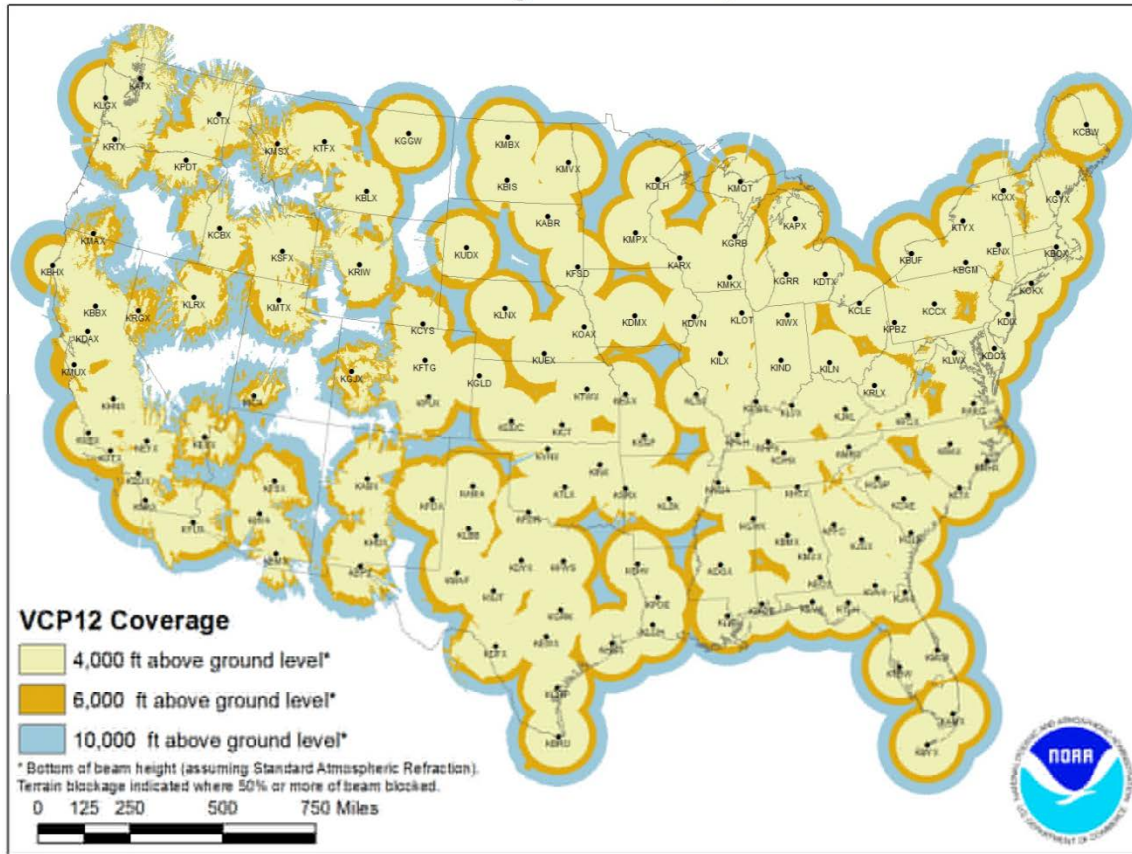
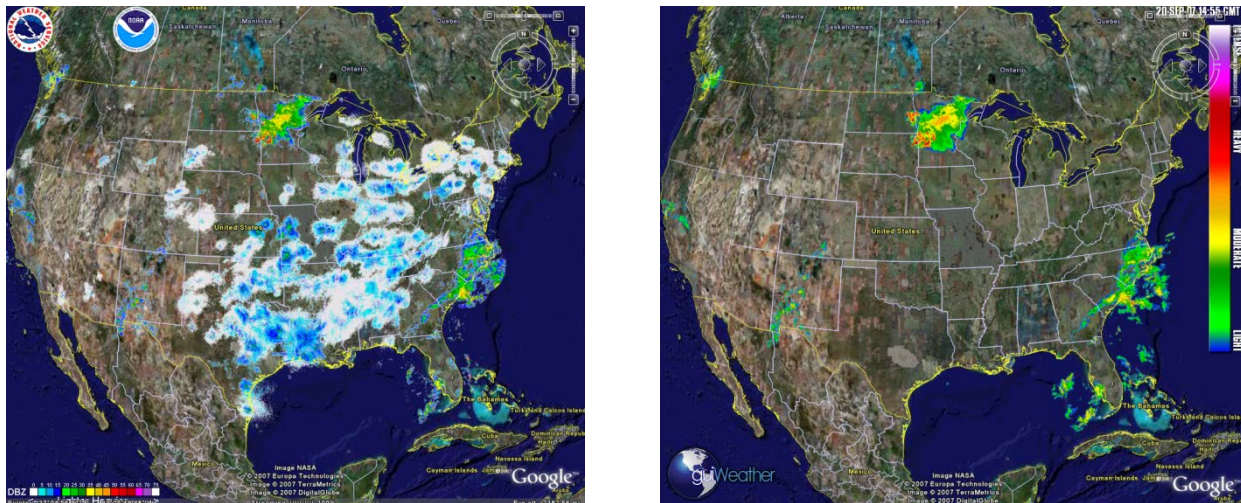


Figure D.3. U.S. radar locations and their radial extents of coverage below 10,000 feet above ground level (AGL). Each U.S. radar covers an approximate 285 mile radial extent over which the radar can detect precipitation.

The WDT and National Severe Storms Lab (NSSL) Radar Data Quality Control Algorithm (RDQC) removes non-precipitation artifacts from base Level-II radar data and remaps the data from polar coordinates to a Cartesian (latitude/longitude) grid. Non-precipitation artifacts include ground clutter, bright banding, sea clutter, anomalous propagation, sun strobes, clear air returns, chaff, biological targets, electronic interference and hardware test patterns. The RDQC algorithm uses sophisticated data processing and a Quality Control Neural Network (QCNN) to delineate the precipitation echoes caused by radar artifacts (Lakshmanan and Valente 2004). Beam blockages

due to terrain are mitigated by using 30 meter DEM data to compute and then discard data from a radar beam that clears the ground by less than 50 meters and incurs more than 50% power blockage. A clear-air echo removal scheme is applied to radars in clear-air mode when there is no precipitation reported from observation gauges within the vicinity of the radar. In areas of radar coverage overlap, a distance weighting scheme is applied to assign reflectivity to each grid cell, for multiple vertical levels. This scheme is applied to data from the nearest radar that is unblocked by terrain.

Once the data from individual radars have passed through the RDQC, they are merged to create a seamless mosaic for the United States and southern Canada as shown in Figure D.4. A multi-sensor quality control can be applied by post-processing the mosaic to remove any remaining “false echoes”. This technique uses observations of infra-red cloud top temperatures by GOES satellite and surface temperature to create a precipitation/no-precipitation mask. Figure 4 shows the impact of WDT’s quality control measures. Upon completing all QC, WDT converts the radar data from its native polar coordinate projection (1 degree x 1.0 km) into a longitude-latitude Cartesian grid (based on the WGS84 datum), at a spatial resolution of $\sim 1/3^{\text{rd}}$ mi² for processing in SPAS.



a) b)
Figure D.4. (a) Level-II radar mosaic of CONUS radar with no quality control, (b) WDT quality controlled Level-II radar mosaic.

SPAS conducts further QC on the radar mosaic by infilling areas contaminated by beam blockages. Beam blocked areas are objectively determined by evaluating total storm reflectivity grid which naturally amplifies areas of the SPAS analysis domain suffering from beam blockage as shown in Figure D.5.

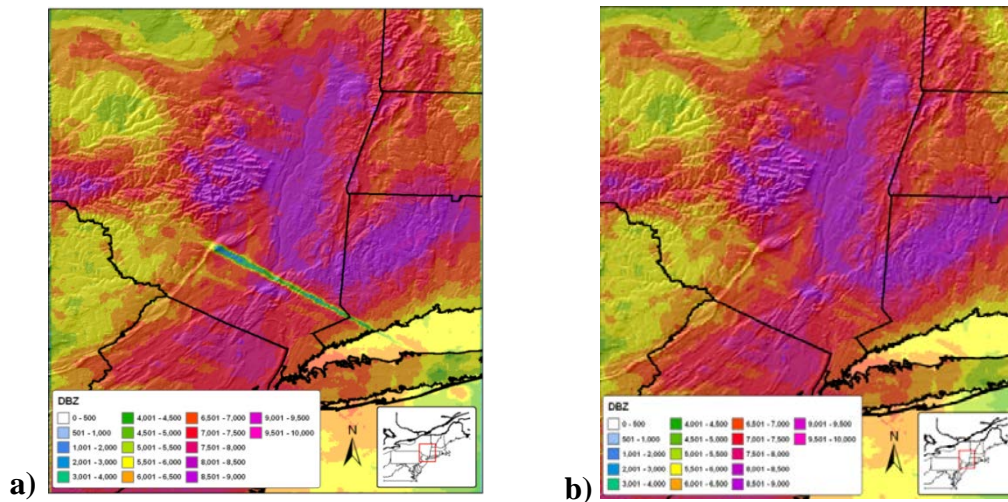


Figure D.5. Illustration of SPAS-beam blockage infilling where (a) is raw, blocked radar and (b) is filled for a 42-hour storm event.

METHODOLOGY

Daily and Supplemental Precipitation to Hourly

To obtain one hour temporal resolutions and utilize all gauge data, it is necessary to disaggregate the daily and supplemental precipitation observations into estimated hourly amounts. This process has traditionally been accomplished by distributing (temporally) the precipitation at each daily/supplemental gauge in accordance to a single nearby hourly gauge (Thiessen polygon approach). However, this may introduce biases and not correctly represent hourly precipitation at daily/supplemental gauges situated in-between hourly gauges. Instead, SPAS uses a spatial approach by which the estimated hourly precipitation at each daily and supplemental gauge is governed by a distance weighted algorithm of all nearby true hourly gauges.

To disaggregate (i.e. distribute) daily/supplemental gauge data into estimate hourly values, the true hourly gauge data are first evaluated and quality controlled using synoptic maps, nearby gauges, orographic effects, gauge history and other documentation on the storm. Any problems with the hourly data are resolved, and when possible/necessary accumulated hourly values are distributed. If an hourly value is missing, the analyst can choose to either estimate it or leave it missing for SPAS to estimate later based on nearby hourly gauges. At this point in the process, pseudo (hourly) gauges can be added to represent precipitation timing in topographically complex locations, areas with limited/no hourly data or to capture localized convection. To adequately capture the temporal variations of the precipitation, a pseudo hourly gauge is sometimes necessary. A pseudo gauge is created by distributing the precipitation at a co-located daily gauge or by creating a completely new pseudo gauge from other information such as inferences from COOP observation forms, METAR visibility data (if hourly precipitation are not already available), lightning data, satellite data, or

radar data. Often radar data are the best/only choice for creating pseudo hourly gauges, but this is done cautiously given the potential differences (over-shooting of the radar beam equating to erroneous precipitation) between radar data and precipitation. In any case, the pseudo hourly gauge is flagged so SPAS only uses it for timing and not magnitude. Care is taken to ensure hourly pseudo gauges represent justifiably important physical and meteorological characteristics before being incorporated into the SPAS database. Although pseudo gauges provide a very important role, their use is kept to a minimum. The importance of insuring the reliability of every hourly gauge cannot be over emphasized. All of the final hourly gauge data, including pseudos, are included in the hourly SPAS precipitation database.

Using the hourly SPAS precipitation database, each hourly precipitation value is converted into a percentage that represents the incremental hourly precipitation divided by the total SPP precipitation. The GIS-ready x-y-z file is constructed for each hour and it includes the latitude (x), longitude(y) and the percent of precipitation (z) for a particular hour. Using the GRASS GIS, an inverse-distance-weighting squared (IDW) interpolation technique is applied to each of the hourly files. The result is a continuous grid with percentage values for the entire analysis domain, keeping the grid cells on which the hourly gauge resides faithful to the observed/actual percentage. Since the percentages typically have a high degree of spatial autocorrelation, the spatial interpolation has skill in determining the percentages between gauges, especially since the percentages are somewhat independent of the precipitation magnitude. The end result is a GIS grid for each hour that represents the percentage of the SPP precipitation that fell during that hour.

After the hourly percentage grids are generated and QCed for the entire SPP, a program is executed that converts the daily/supplemental gauge data into incremental hourly data. The timing at each of the daily/supplemental gauges is based on (1) the daily/supplemental gauge observation time, (2) daily/supplemental precipitation amount and (3) the series of interpolated hourly percentages extracted from grids (described above).

This procedure is detailed in Figure D.6 below. In this example, a supplemental gauge reported 1.40” of precipitation during the storm event and is located equal distance from the three surrounding hourly recording gauges. The procedure steps are:

- Step 1. For each hour, extract the percent of SPP from the hourly gauge-based percentage at the location of the daily/supplemental gauge. In this example, assume these values are the average of all the hourly gauges.
- Step 2. Multiply the individual hourly percentages by the total storm precipitation at the daily/supplemental gauge to arrive at estimated hourly precipitation at the daily/supplemental gauge. To make the daily/supplemental accumulated precipitation data faithful to the daily/supplemental observations, it is sometimes

necessary to adjust the hourly percentages so they add up to 100% and account for 100% of the daily observed precipitation.

Hour								
Precipitation	1	2	3	4	5	6	Total	
Hourly station 1	0.02	0.12	0.42	0.50	0.10	0.00	1.16	
Hourly station 2	0.01	0.15	0.48	0.62	0.05	0.01	1.32	
Hourly station 3	0.00	0.18	0.38	0.55	0.20	0.05	1.36	
Hour								
Percent of total storm precip.	1	2	3	4	5	6	Total	
Hourly station 1	2%	10%	36%	43%	9%	0%	100%	
Hourly station 2	1%	11%	36%	47%	4%	1%	100%	
Hourly station 3	0%	13%	28%	40%	15%	4%	100%	
<i>Average</i>	1%	12%	34%	44%	9%	1%	100%	
Storm total precipitation at daily gauge				1.40				
Hour								
Precipitation (estimated)	1	2	3	4	5	6	Total	
Daily station	0.01	0.16	0.47	0.61	0.13	0.02	1.40	

Figure D.6 Example of disaggregation of daily precipitation into estimated hourly precipitation based on three (3) surrounding hourly recording gauges.

In cases where the hourly grids do not indicate any precipitation falling during the daily/supplemental gauge observational period, yet the daily/supplemental gauge reported precipitation, the daily/supplemental total precipitation is evenly distributed throughout the hours that make up the observational period; although this does not happen very often, this solution is consistent with NWS procedures. However, the SPAS analyst is notified of these cases in a comprehensive log file, and in most cases they are resolvable, sometimes with a pseudo hourly gauge.

GAUGE QUALITY CONTROL

Exhaustive quality control measures are taken throughout the SPAS analysis. Below are a few of the most significant QC measures taken.

Mass Curve Check

A mass curve-based QC-methodology is used to ensure the timing of precipitation at all gauges is consistent with nearby gauges. SPAS groups each gauge with the nearest four gauges (regardless of type) into a single file. These files are subsequently used in software for graphing and evaluation. Unusual characteristics in the mass curve are investigated and the gauge data corrected, if possible and warranted. See Figure E.7 for an example.

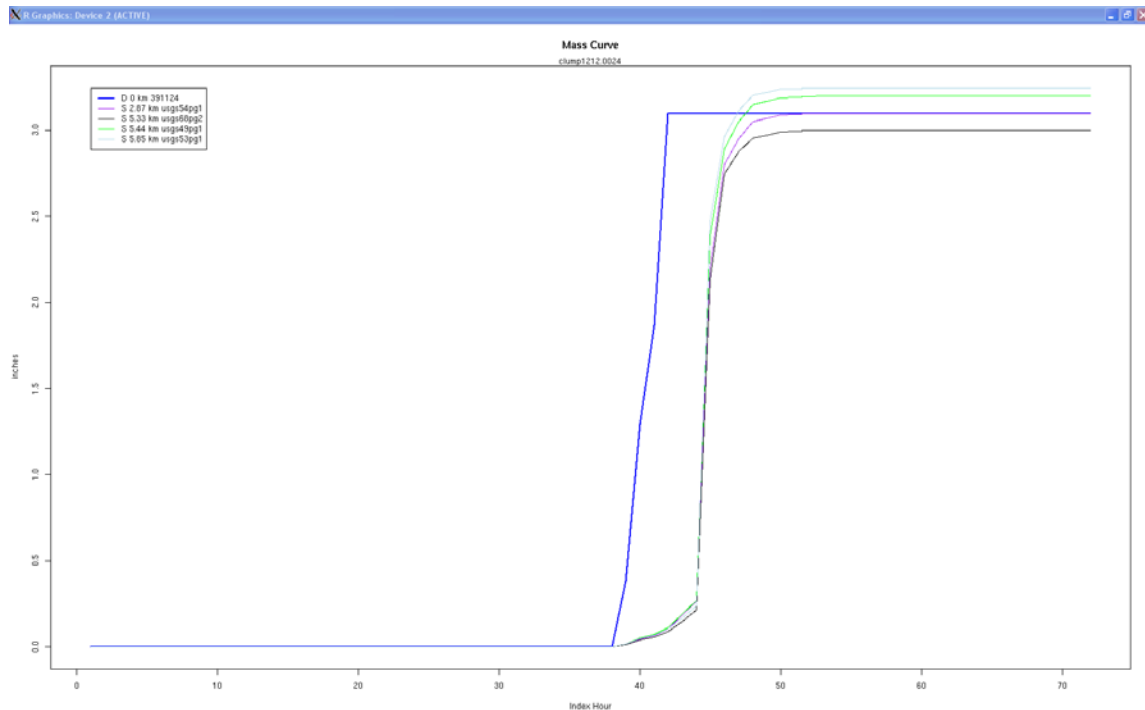


Figure D.7 Sample mass curve plot depicting a precipitation gauge with an erroneous observation time (blue line). X-axis is the SPAS index hour and the y-axis is inches. The statistics in the upper left denote gauge type, distance from target gauge (in km), and gauge ID. In this example, the center gauge (blue line) was found to have an observation error/shift of 1 day.

Gauge Mis-location Check

Although the gauge elevation is not explicitly used in SPAS, it is however used as a means of QCing gauge location. Gauge elevations are compared to a high-resolution 15-second DEM to identify gauges with large differences, which may indicate erroneous longitude and/or latitude values.

Co-located Gauge QC

Care is also taken to establish the most accurate precipitation depths at all co-located gauges. In general, where a co-located gauge pair exists, the highest precipitation is accepted (if deemed accurate). If the hourly gauge reports higher precipitation, then the co-located daily (or supplemental) is removed from the analysis since it would not add anything to the analysis. Often daily (or supplemental) gauges report greater precipitation than a co-located hourly station since hourly tipping bucket gauges tend to suffer from gauge under-catch, particularly during extreme events, due to loss of precipitation during tips. In these cases the daily/supplemental is retained for the magnitude and the hourly used as a pseudo hourly gauge for timing. Large discrepancies between any co-located gauges are investigated and resolved since SPAS can only utilize a single gauge magnitude at each co-located site.

SPATIAL INTERPOLATION

At this point the QCed observed hourly and disaggregated daily/supplemental hourly precipitation data are spatially interpolated into hourly precipitation grids. SPAS has three options for conducting the hourly precipitation interpolation, depending on the terrain and availability of radar data, thereby allowing SPAS to be optimized for any particular storm type or location. Figure D.8 depicts the results of each spatial interpolation methodology based on the same precipitation gauge data.

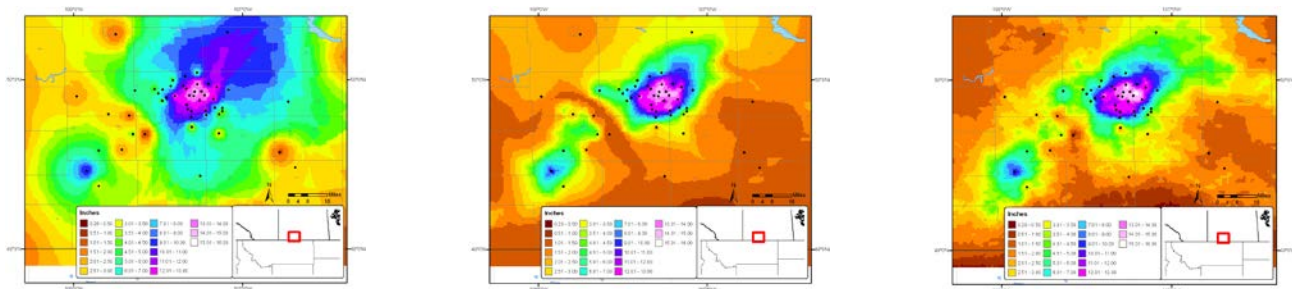


Figure D.8. Depictions of total storm precipitation based on the three SPAS interpolation methodologies for a storm (SPAS #1177, Vanguard, Canada) across flat terrain: (a) no basemap, (b) basemap-aided and (c) radar.

Basic Approach

The basic approach interpolates the hourly precipitation point values to a grid using an inverse distance weighting squared GIS algorithm. This is sometimes the best choice for convective storms over flat terrain when radar data are not available, yet high gauge density instills reliable precipitation patterns. This approach is rarely used.

Basemap Approach

Another option includes use of a “basemap”, also known as a climatologically-aided interpolation (Hunter 2005). As noted before, the spatial patterns of the basemap govern the interpolation between points of hourly precipitation estimates, while the actual hourly precipitation values govern the magnitude. This approach to interpolating point data across complex terrain is widely used. In fact, it was used extensively by the NWS during their storm analysis era from the 1940s through the 1970s (USACE 1973, Hansen et al. 1988, Corrigan et al. 1999).

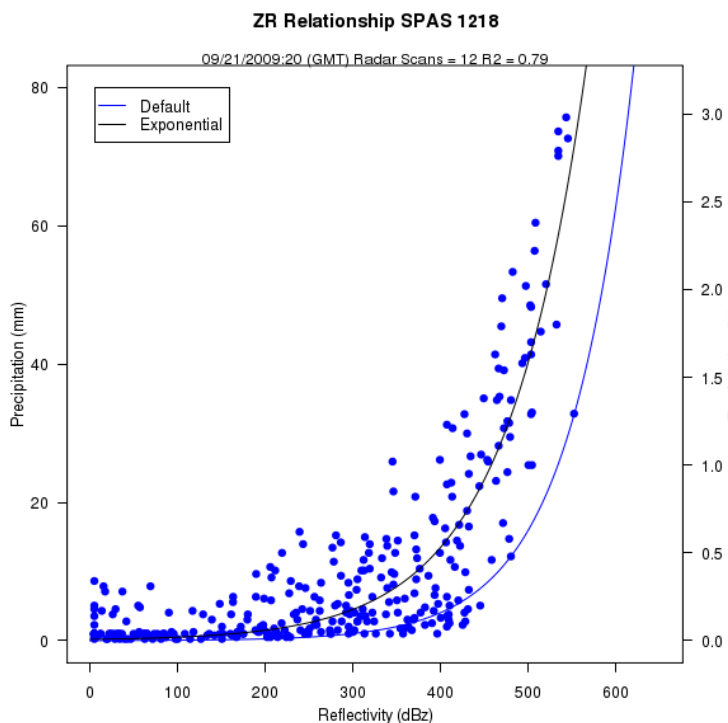
In application, the hourly precipitation gauge values are first normalized by the corresponding grid cell value of the basemap before being interpolated. The normalization allows information and knowledge from the basemap to be transferred to the spatial distribution of the hourly precipitation. Using an IDW squared algorithm, the normalized hourly precipitation values are interpolated to a grid. The resulting grid is then multiplied by the basemap grid to produce the hourly precipitation grid. This is repeated each hour of the storm.

Radar Approach

The coupling of SPAS with NEXRAD provides the most accurate method of spatially and temporally distributing precipitation. To increase the accuracy of the results however, quality-controlled precipitation observations are used for calibrating the radar reflectivity to rain rate relationship (Z-R relationship) each hour instead of assuming a default Z-R relationship. Also, spatial variability in the Z-R relationship is accounted for through local bias corrections (described later). The radar approach involves several steps, each briefly described below. The radar approach cannot operate alone – either the basic or basemap approach must be completed before radar data can be incorporated.

Z-R Relationship

SPAS derives high quality precipitation estimates by relating quality controlled level-II NEXRAD radar reflectivity radar data with quality-controlled precipitation gauge data to calibrate the Z-R (radar reflectivity, Z, and precipitation, R) relationship. Optimizing the Z-R relationship is essential for capturing temporal changes in the Z-R. Most current radar-derived precipitation techniques rely on a constant relationship between radar reflectivity and precipitation rate for a given storm type (e.g. tropical, convective), vertical structure of reflectivity and/or reflectivity magnitudes. This non-linear relationship is described by the Z-R equation below:



$$Z = A R^b \quad (1)$$

Figure D.9. Example SPAS (denoted as “Exponential”) vs. default Z-R relationship (SPAS #1218, Georgia September 2009).

Where Z is the radar reflectivity (measured in units of dBZ), R is the precipitation (precipitation) rate (millimeters per hour), A is the “multiplicative coefficient” and b is the “power coefficient”. Both A and b are directly related to the rain drop size distribution (DSD) and rain drop number distribution (DND) within a cloud (Martner and Dubovskiy 2005). The variability in the results of Z versus R is a direct result of differing DSD, DND and air mass characteristics (Dickens 2003). The DSD and DND are determined by complex interactions of microphysical processes that fluctuate regionally, seasonally, daily, hourly, and even within the same cloud. For these reasons, SPAS calculates an optimized Z - R relationship across the analysis domain each hour, based on observed precipitation rates and radar reflectivity (see Figure D.9).

The National Weather Service (NWS) utilizes different default Z - R algorithms, depending on the type of precipitation event, to estimate precipitation from NEXRAD radar reflectivity data across the United States (see Figure D.10) (Baeck and Smith 1998 and Hunter 1999). A default Z - R relationship of $Z = 300R^{1.4}$ is the primary algorithm used throughout the continental U.S. However, it is widely known that this, compared to unadjusted radar-aided estimates of precipitation, suffers from deficiencies that may lead to significant over or under-estimation of precipitation.

RELATIONSHIP	Optimum for:	Also recommended for:
Marshall-Palmer ($z=200R^{1.6}$)	General stratiform precipitation	
East-Cool Stratiform ($z=130R^{2.0}$)	Winter stratiform precipitation - east of continental divide	Orographic rain - East
West-Cool Stratiform ($z=75R^{2.0}$)	Winter stratiform precipitation - west of continental divide	Orographic rain - West
WSR-88D Convective ($z=300R^{1.4}$)	Summer deep convection	Other non-tropical convection
Rosenfeld Tropical ($z=250R^{1.2}$)	Tropical convective systems	

Figure D.10. Commonly used Z-R algorithms used by the NWS.

Instead of adopting a standard Z - R , SPAS utilizes a least squares fit procedure for optimizing the Z - R relationship each hour of the SPP. The process begins by determining if sufficient (minimum 12) observed hourly precipitation and radar data pairs are available to compute a reliable Z - R . If insufficient (<12) gauge pairs are available, then SPAS adopts the previous hour Z - R relationship, if available, or applies a user-defined default Z - R algorithm from Figure 9. If sufficient data are available, the one hour sum of NEXRAD reflectivity (Z) is related to the 1-hour precipitation at each gauge. A least-squares-fit exponential function using the data points is computed. The resulting best-fit, one hour-based Z - R is subjected to several tests to determine if the Z - R relationship and its resulting precipitation rates are within a certain tolerance based on the R-squared fit measure and difference between the derived and default Z - R precipitation results.

Experience has shown the actual Z-R versus the default Z-R can be significantly different (Figure D.11). These Z-R relationships vary by storm type and location. A standard output of all SPAS analyses utilizing NEXRAD includes a file with each hour's adjusted Z-R relationship as calculated through the SPAS program.

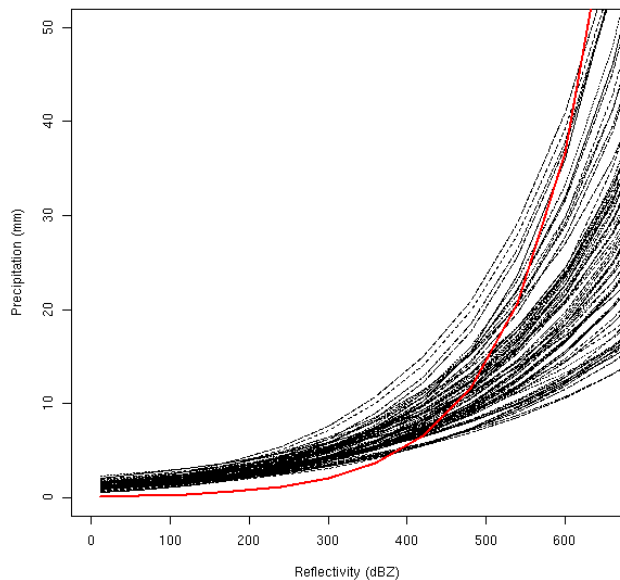


Figure D.11. Comparison of the SPAS optimized hourly Z-R relationships (black lines) versus a default $Z=75R^{2.0}$ Z-R relationship (red line) for a period of 99 hours for a storm over southern California.

Radar-aided Hourly Precipitation Grids

Once a mathematically optimized hourly Z-R relationship is determined, it is applied to the total hourly Z grid to compute an initial precipitation rate (inches/hour) at each grid cell. To account for spatial differences in the Z-R relationship, SPAS computes residuals, the difference between the initial precipitation analysis (via the Z-R equation) and the actual “ground truth” precipitation (observed – initial analysis), at each gauge. The point residuals, also referred to as local biases, are normalized and interpolated to a residual grid using an inverse distance squared weighting algorithm. A radar-based hourly precipitation grid is created by adding the residual grid to the initial grid; this allows the precipitation at the grid cells for which gauges are “on” to be true and faithful to the gauge measurement. The pre-final radar-aided precipitation grid is subject to some final, visual QC checks to ensure the precipitation patterns are consistent with the terrain; these checks are particularly important in areas of complex terrain where even QCed radar data can be unreliable. The next incremental improvement with SPAS program will come as the NEXRAD radar sites are upgraded to dual-polarimetric capability.

Radar- and Basemap-Aided Hourly Precipitation Grids

At this stage of the radar approach, a radar- and basemap-aided hourly precipitation grid exists for each hour. At locations with precipitation gauges, the grids are equal, however elsewhere the grids can vary for a number of reasons. For instance, the basemap-aided hourly precipitation grid may depict heavy precipitation in an area of complex terrain, blocked by the radar, whereas the radar-aided hourly precipitation grid may suggest little, if any, precipitation fell in the same area. Similarly, the radar-aided hourly precipitation grid may depict an area of heavy precipitation in flat terrain that the basemap-approach missed since the area of heavy precipitation occurred in an area without gauges. SPAS uses an algorithm to compute the hourly precipitation at each pixel given the two results. Areas that are completely blocked from a radar signal are accounted for with the basemap-aided results (discussed earlier). Precipitation in areas with orographically effective terrain and reliable radar data are governed by a blend of the basemap- and radar-aided precipitation. Elsewhere, the radar-aided precipitation is used exclusively. This blended approach has proven effective for resolving precipitation in complex terrain, yet retaining accurate radar-aided precipitation across areas where radar data are reliable. Figure D.12 illustrates the evolution of final precipitation from radar reflectivity in an area of complex terrain in southern California.

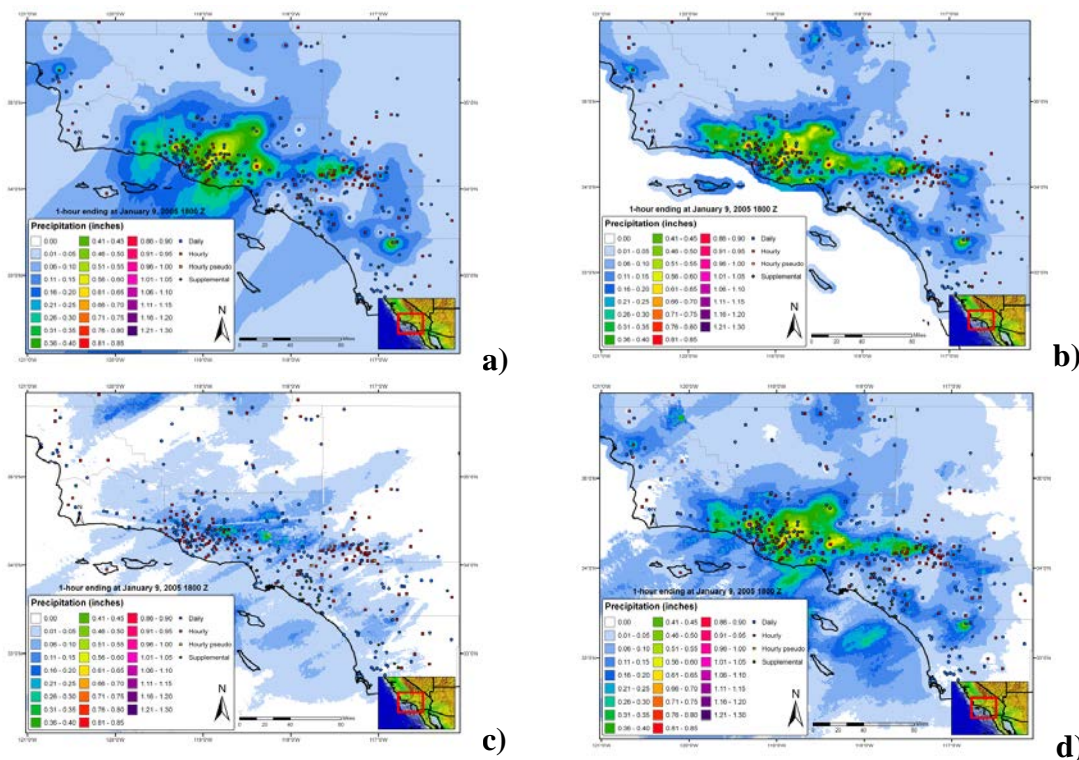


Figure D.12. A series of maps depicting 1-hour of precipitation utilizing (a) inverse distance weighting of gauge precipitation, (b) gauge data together with a climatologically-aided interpolation scheme, (c) default Z-R radar-estimated interpolation (no gauge correction) and (d) SPAS precipitation for a January 2005 storm in southern California, USA.

SPAS versus Gauge Precipitation

Performance measures are computed and evaluated each hour to detect errors and inconsistencies in the analysis. The measures include: hourly Z-R coefficients, observed hourly maximum precipitation, maximum gridded precipitation, hourly bias, hourly mean absolute error (MAE), root mean square error (RMSE), and hourly coefficient of determination (r^2).

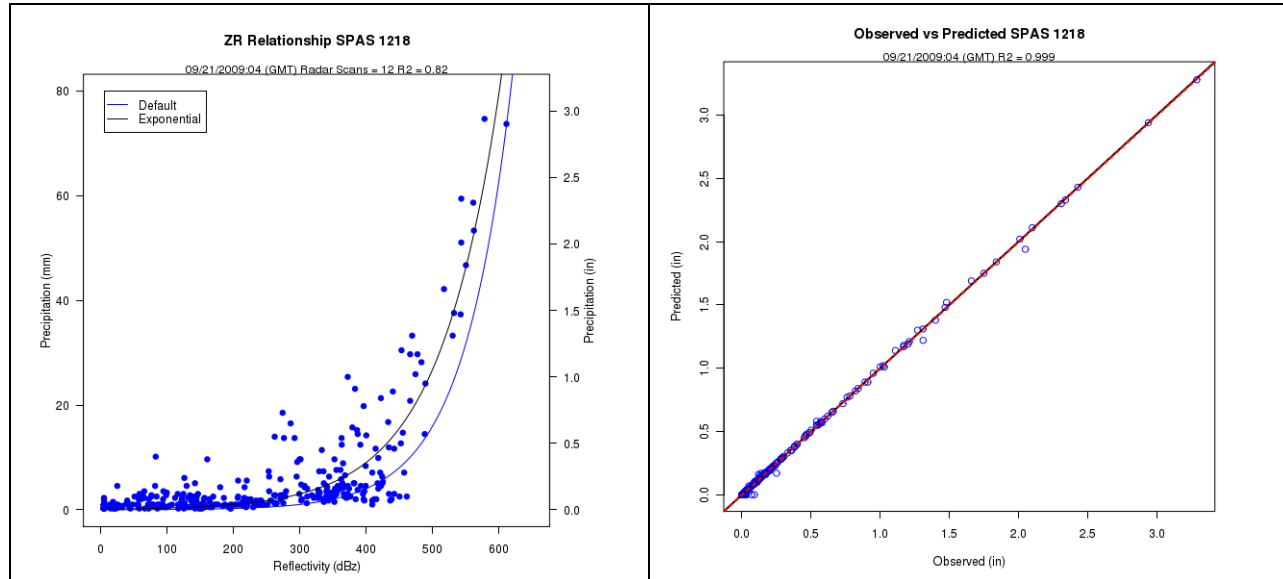


Figure D.13. Z-R plot (a), where the blue line is the SPAS derived Z-R and the black line is the default Z-R, and the (b) associated observed versus SPAS scatter plot at gauge locations.

Comparing SPAS-calculated precipitation (R_{spas}) to observed point precipitation depths at the gauge locations provides an objective measure of the consistency, accuracy and bias. Generally speaking SPAS is usually within 5% of the observed precipitation (see Figure D.13). Less-than-perfect correlations between SPAS precipitation depths and observed precipitation at gauged locations could be the result of any number of issues, including:

- **Point versus area:** A rain gauge observation represents a much smaller area than the area sampled by the radar. The area that the radar is sampling is approximately 1 km^2 , whereas a standard rain gauge has an opening 8 inches in diameter, hence it only samples approximately $8.0 \times 10^{-9} \text{ km}^2$. Furthermore, the radar data represents an average reflectivity (Z) over the grid cell, when in fact the reflectivity can vary across the 1 km^2 grid cell. Therefore, comparing a grid cell radar derived precipitation value to a gauge (point) precipitation depth measured may vary.
- **Precipitation gauge under-catch:** Although we consider gauge data “ground truth,” we recognize gauges themselves suffer from inaccuracies. Precipitation gauges, shielded and

unshielded, inherently underestimate total precipitation due to local airflow, wind under-catch, wetting, and evaporation. The wind under-catch errors are usually around 5% but can be as large as 40% in high winds (Guo et al. 2001, Duchon and Essenberg 2001, Ciach 2003, Tokay et al. 2010). Tipping buckets miss a small amount of precipitation during each tip of the bucket due to the bucket travel and tip time. As precipitation intensities increase, the volumetric loss of precipitation due to tipping tends to increase. Smaller tipping buckets can have higher volumetric losses due to higher tip frequencies, but on the other hand capture higher precision timing.

- **Radar Calibration:** NEXRAD radars calibrate reflectivity every volume scan, using an internally generated test. The test determines changes in internal variables such as beam power and path loss of the receiver signal processor since the last off-line calibration. If this value becomes large, it is likely that there is a radar calibration error that will translate into less reliable precipitation estimates. The calibration test is supposed to maintain a reflectivity precision of 1 dBZ. A 1 dBZ error can result in an error of up to 17% in R_{spas} using the default Z-R relationship $Z=300R^{1.4}$. Higher calibration errors will result in higher R_{spas} errors. However, by performing correlations each hour, the calibration issue is minimized in SPAS.
- **Attenuation:** Attenuation is the reduction in power of the radar beams' energy as it travels from the antenna to the target and back. It is caused by the absorption and the scattering of power from the beam by precipitation. Attenuation can result in errors in Z as large as 1 dBZ especially when the radar beam is sampling a large area of heavy precipitation. In some cases, storm precipitation is so intense (>12 inches/hour) that individual storm cells become "opaque" and the radar beam is totally attenuated. Armed with sufficient gauge data however, SPAS will overcome attenuation issues.
- **Range effects:** The curvature of the Earth and radar beam refraction result in the radar beam becoming more elevated above the surface with increasing range. With the increased elevation of the radar beam comes a decrease in Z values due to the radar beam not sampling the main precipitation portion of the cloud (i.e. "over topping" the precipitation and/or cloud altogether). Additionally, as the radar beam gets further from the radar, it naturally samples a larger and larger area, therefore amplifying point versus area differences (described above).
- **Radar Beam Occultation/Ground Clutter:** Radar occultation (beam blockage) results when the radar beam's energy intersects terrain features as depicted in Figure D.14. The result is an increase in radar reflectivity values that can result in higher than normal precipitation estimates. The WDT processing algorithms account for these issues, but SPAS

uses GIS spatial interpolation functions to infill areas suffering from poor or no radar coverage.

- **Anomalous Propagation (AP):** AP is false reflectivity echoes produced by unusual rates of refraction in the atmosphere. WDT algorithms remove most of the AP and false echoes, however in extreme cases the air near the ground may be so cold and dense that a radar beam that starts out moving upward is bent all the way down to the ground. This produces erroneously strong echoes at large distances from the radar. Again, equipped with sufficient gauge data, the SPAS bias corrections will overcome AP issues.

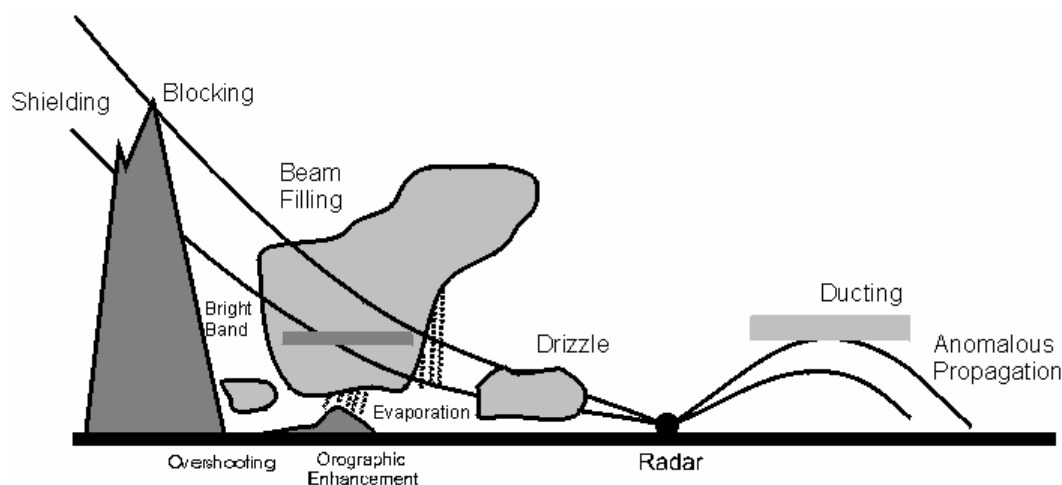


Figure D.14 Depiction of radar artifacts. (Source: Wikipedia)

SPAS is designed to overcome many of these short-comings by carefully using radar data for defining the spatial patterns and relative magnitudes of precipitation, but allowing measured precipitation values (“ground truth”) at gauges to govern the magnitude. When absolutely necessary, the observed precipitation values at gauges are nudged up (or down) to force SPAS results to be consistent with observed gauge values. Nudging gauge precipitation values helps to promote better consistency between the gauge value and the gridcell value, even though these two values sometimes should not be the same since they are sampling different area sizes. For reasons discussed in the “SPAS versus Gauge Precipitation” section, the gauge value and gridcell value can vary. Plus, SPAS is designed to toss observed individual hourly values that are grossly inconsistent with radar data, hence driving a difference between the gauge and gridcell. In general, when the gauge and gridcell value differ by more than 15% and/or 0.50 inches, and the gauge data have been validated, then it is justified to artificially increase or decrease slightly the observed gauge value to “force” SPAS to derive a gridcell value equal to the observed value. Sometimes simply shifting the gauge location to an adjacent gridcell resolves the problems. Regardless, a large gauge versus gridcell difference is a “red flag” and sometimes the result of an erroneous gauge value or a mis-

located gauge, but in some cases the difference can only be resolved by altering the precipitation value.

Before results are finalized, a precipitation intensity check is conducted to ensure the spatial patterns and magnitudes of the maximum storm intensities at 1-, 6-, 12-, etc. hours are consistent with surrounding gauges and published reports. Any erroneous data are corrected and SPAS re-run. Considering all of the QA/QC checks in SPAS, it typically requires 5-15 basemap SPAS runs and, if radar data are available, another 5-15 radar-aided runs, to arrive at the final output.

Test Cases

To check the accuracy of the DAD software, three test cases were evaluated.

“Pyramidville” Storm

The first test was that of a theoretical storm with a pyramid shaped isohyetal pattern. This case was called the Pyramidville storm. It contained 361 hourly stations, each occupying a single grid cell. The configuration of the Pyramidville storm (see Figure D.15) allowed for uncomplicated and accurate calculation of the analytical DA truth independent of the DAD software. The main motivation of this case was to verify that the DAD software was properly computing the area sizes and average depths.

1. Storm center: 39°N 104°W
2. Duration: 10-hours
3. Maximum grid cell precipitation: 1.00”
4. Grid cell resolution: 0.06 sq.-miles (361 total cells)
5. Total storm size: 23.11 sq-miles
6. Distribution of precipitation:
 - Hour 1: Storm drops 0.10” at center (area 0.06 sq-miles)
 - Hour 2: Storm drops 0.10” over center grid cell AND over one cell width around hour 1 center
 - Hours 3-10:
 1. Storm drops 0.10” per hour at previously wet area, plus one cell width around previously wet area
 2. Area analyzed at every 0.10”
 3. Analysis resolution: 15-sec (~.25 square miles)

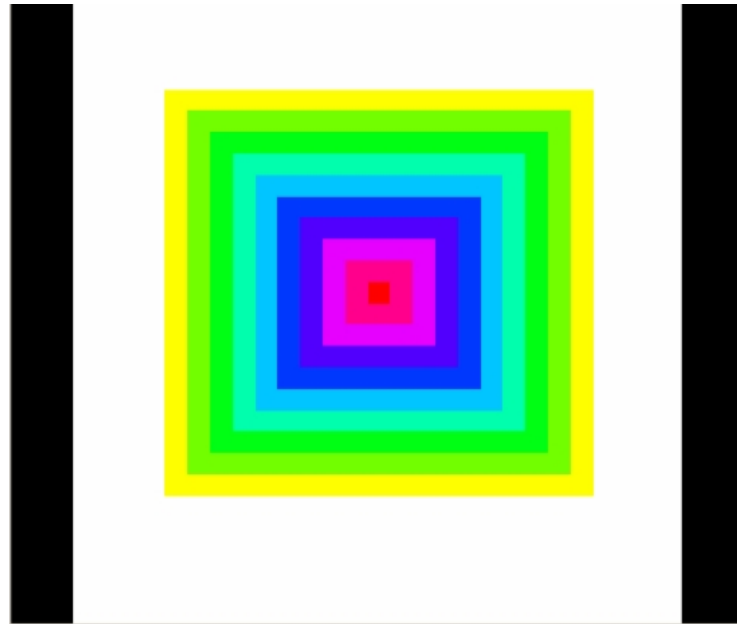


Figure D.15 “Pyramidville” Total precipitation. Center = 1.00”, Outside edge = 0.10”.

The analytical truth was calculated independent of the DAD software, and then compared to the DAD output. The DAD software results were equal to the truth, thus demonstrating that the DA estimates were properly calculated (Figure D.16).

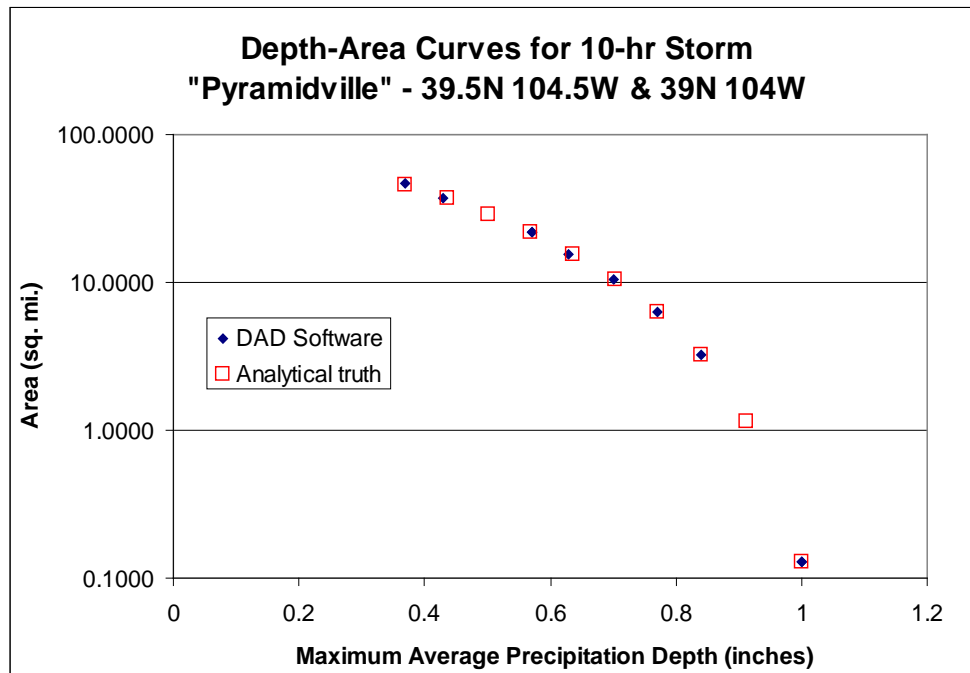


Figure D.16 10-hour DA results for “Pyramidville”; truth vs. output from DAD software.

The Pyramidville storm was then changed such that the mass curve and spatial interpolation methods would be stressed. Test cases included:

- Two-centers, each center with 361 hourly stations
- A single center with 36 hourly stations, 0 daily stations
- A single center with 3 hourly stations and 33 daily stations

As expected, results began shifting from the ‘truth,’ but minimally and within the expected uncertainty.

Ritter, Iowa Storm, June 7, 1953

Ritter, Iowa was chosen as a test case for a number of reasons. The NWS had completed a storm analysis, with available DAD values for comparison. The storm occurred over relatively flat terrain, so orographics were not an issue. An extensive “bucket survey” provided a great number of additional observations from this event. Of the hundreds of additional reports, about 30 of the most accurate reports were included in the DAD analysis.

The DAD software results are very similar to the NWS DAD values (Table D.2).

Table D.2. The percent difference [(AWA-NWS)/NWS] between the AWA DA results and those published by the NWS for the 1953 Ritter, Iowa storm.

% Difference

Area (sq.mi.)	Duration (hours)				total
	6	12	24		
10	-15%	-7%	2%	2%	
100	-7%	-6%	1%	1%	
200	2%	0%	9%	9%	
1000	-6%	-7%	4%	4%	
5000	-13%	-8%	2%	2%	
10000	-14%	-6%	0%	0%	

Westfield, Massachusetts Storm, August 8, 1955

Westfield, Massachusetts was also chosen as a test case for a number of reasons. It is a probable maximum precipitation (PMP) driver for the northeastern United States. Also, the Westfield storm was analyzed by the NWS and the DAD values are available for comparison. Although this case proved to be more challenging than any of the others, the final results are very similar to those published by the NWS (Table D.3).

Table D.3. The percent difference [(AWA-NWS)/NWS] between the AWA DA results and those published by the NWS for the 1955 Westfield, Massachusetts storm.

% Difference

Area (sq. mi.)	Duration (hours)							
	6	12	24	36	48	60	total	
10	2%	3%	0%	1%	-1%	0%	2%	
100	-5%	2%	4%	-2%	-6%	-4%	-3%	
200	-6%	1%	1%	-4%	-7%	-5%	-5%	
1000	-4%	-2%	1%	-6%	-7%	-6%	-3%	
5000	3%	2%	-3%	-3%	-5%	-5%	0%	
10000	4%	9%	-5%	-4%	-7%	-5%	1%	
20000	7%	12%	-6%	-3%	-4%	-3%	3%	

The primary components of SPAS are: storm search, data extraction, quality control (QC), conversion of daily precipitation data into estimated hourly data, hourly and total storm precipitation grids/maps and a complete storm-centered DAD analysis.

OUTPUT

Armed with accurate, high-resolution precipitation grids, a variety of customized output can be created (see Figures D.17A-D). Among the most useful outputs are sub-hourly precipitation grids for input into hydrologic models. Sub-hourly (i.e. 5-minute) precipitation grids are created by applying the appropriate optimized hourly Z-R (scaled down to be applicable for instantaneous Z) to each of the individual 5-minute radar scans; 5-minutes is often the native scan rate of the radar in the US. Once the scaled Z-R is applied to each radar scan, the resulting precipitation is summed up. The proportion of each 5-minute precipitation to the total 1-hour radar-aided precipitation is calculated. Each 5-minute proportion (%) is then applied to the quality controlled, bias corrected 1-hour total precipitation (created above) to arrive at the final 5-minute precipitation for each scan. This technique ensures the sum of 5-minute precipitation equals that of the quality controlled, bias corrected 1-hour total precipitation derived initially.

Depth-area-duration (DAD) tables/plots, shown in Figure D.17d, are computed using a highly-computational extension to SPAS. DADs provide an objective three dimensional (magnitude, area size, and duration) perspective of a storms' precipitation. SPAS DADs are computed using the procedures outlined by the NWS Technical Paper 1 (1946).

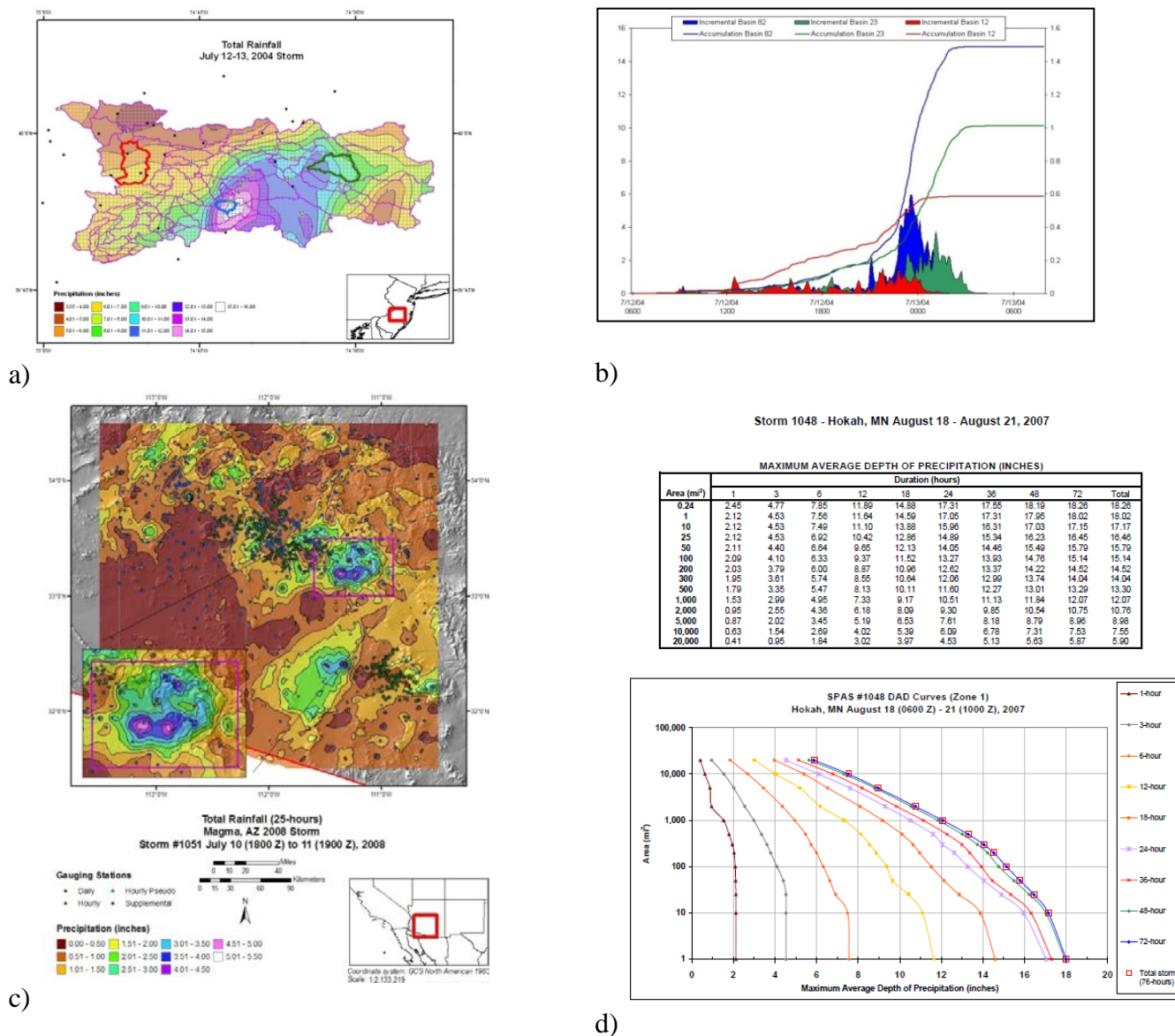


Figure D.17. Various examples of SPAS output, including (a) total storm map and its associated (b) basin average precipitation time series, (c) total storm precipitation map, (d) depth-area-duration (DAD) table and plot.

SUMMARY

Grounded on years of scientific research with a demonstrated reliability in post-storm analyses, SPAS is a hydro-meteorological tool that provides accurate precipitation analyses for a variety of applications. SPAS has the ability to compute precise and accurate results by using sophisticated timing algorithms, “basemaps”, a variety of precipitation data and most importantly NEXRAD weather radar data (if available). The approach taken by SPAS relies on hourly, daily and

supplemental precipitation gauge observations to provide quantification of the precipitation amounts while relying on basemaps and NEXRAD data (if available) to provide the spatial distribution of precipitation between precipitation gauge sites. By determining the most appropriate coefficients for the Z-R equation on an hourly basis, the approach anchors the precipitation amounts to accepted precipitation gauge data while using the NEXRAD data to distribute precipitation between precipitation gauges for each hour of the storm. Hourly Z-R coefficient computations address changes in the cloud microphysics and storm characteristics as the storm evolves. Areas suffering from limited or no radar coverage are estimated using the spatial patterns and magnitudes of the independently created basemap precipitation grids. Although largely automated, SPAS is flexible enough to allow hydro-meteorologists to make important adjustments and adapt to any storm situation.

REFERENCES

- Baack M.L., Smith J.A., 1998: “Precipitation Estimation by the WSR-88D for Heavy Precipitation Events”, *Weather and Forecasting*: Vol. 13, No. 2, pp. 416–436.
- Ciach, G.J., 2003: Local Random Errors in Tipping-Bucket Rain Gauge Measurements. *J. Atmos. Oceanic Technol.*, **20**, 752–759.
- Corps of Engineers, U.S. Army, 1945-1973: Storm Rainfall in the United States, Depth-Area-Duration Data. Office of Chief of Engineers, Washington, D.C.
- Corrigan, P., Fenn, D.D., Kluck, D.R., and J.L. Vogel, 1999: Probable Maximum Precipitation Estimates for California. *Hydrometeorological Report No. 59*, U.S. National Weather Service, National Oceanic and Atmospheric Administration, U.S. Department of Commerce, Silver Spring, MD, 392 pp.
- Dickens, J., 2003: “On the Retrieval of Drop Size Distribution by Vertically Pointing Radar”, American Meteorological Society 32nd Radar Meteorology Conference, Albuquerque, NM, October 2005.
- Duchon, C.E., and G.R. Essenberg, 2001: Comparative Precipitation Observations from Pit and Above Ground Rain Gauges with and without Wind Shields, *Water Resources Research*, Vol. 37, N. 12, 3253-3263.
- Faulkner, E., T. Hampton, R.M. Rudolph, and Tomlinson, E.M., 2004: Technological Updates for PMP and PMF – Can They Provide Value for Dam Safety Improvements? Association of State Dam Safety Officials Annual Conference, Phoenix, Arizona, September 26-30, 2004.
- Guo, J. C. Y., Urbonas, B., and Stewart, K., 2001: Rain Catch under Wind and Vegetal Effects. ASCE, *Journal of Hydrologic Engineering*, Vol. 6, No. 1.

- Hansen, E.M., Fenn, D.D., Schreiner, L.C., Stodt, R.W., and J.F., Miller, 1988: Probable Maximum Precipitation Estimates, United States between the Continental Divide and the 103rd Meridian, *Hydrometeorological Report Number 55A*, National weather Service, National Oceanic and Atmospheric Association, U.S. Dept of Commerce, Silver Spring, MD, 242 pp.
- Hunter, R.D. and R.K. Meentemeyer, 2005: Climatologically Aided Mapping of Daily Precipitation and Temperature, *Journal of Applied Meteorology*, October 2005, Vol. 44, pp. 1501-1510.
- Hunter, S.M., 1999: Determining WSR-88D Precipitation Algorithm Performance Using The Stage III Precipitation Processing System, Next Generation Weather Radar Program, WSR-88D Operational Support Facility, Norman, OK.
- Lakshmanan, V. and M. Valente, 2004: Quality control of radar reflectivity data using satellite data and surface observations, 20th Int'l Conf. on Inter. Inf. Proc. Sys. (IIPS) for Meteor., Ocean., and Hydr., Amer. Meteor. Soc., Seattle, CD-ROM, 12.2.
- Martner, B.E, and V. Dubovskiy, 2005: Z-R Relations from Raindrop Disdrometers: Sensitivity To Regression Methods And DSD Data Refinements, 32nd Radar Meteorology Conference, Albuquerque, NM, October, 2005
- Tokay, A., P.G. Bashor, and V.L. McDowell, 2010: Comparison of Rain Gauge Measurements in the Mid-Atlantic Region. *J. Hydrometeor.*, 11, 553-565.
- Tomlinson, E.M., W.D. Kappel, T.W. Parzybok, B. Rappolt, 2006: Use of NEXRAD Weather Radar Data with the Storm Precipitation Analysis System (SPAS) to Provide High Spatial Resolution Hourly Precipitation Analyses for Runoff Model Calibration and Validation, ASDSO Annual Conference, Boston, MA.
- Tomlinson, E.M., and T.W. Parzybok, 2004: Storm Precipitation Analysis System (SPAS), proceedings of Association of Dam Safety Officials Annual Conference, Technical Session II, Phoenix, Arizona.
- Tomlinson, E.M., R.A. Williams, and T.W. Parzybok, September 2003: Site-Specific Probable Maximum Precipitation (PMP) Study for the Great Sacandaga Lake / Stewarts Bridge Drainage Basin, Prepared for Reliant Energy Corporation, Liverpool, New York.
- Tomlinson, E.M., R.A. Williams, and T.W. Parzybok, September 2003: Site-Specific Probable Maximum Precipitation (PMP) Study for the Cherry Creek Drainage Basin, Prepared for the Colorado Water Conservation Board, Denver, CO.
- Tomlinson, E.M., Kappel W.D., Parzybok, T.W., Hultstrand, D., Muhlestein, G., and B. Rappolt, May 2008: Site-Specific Probable Maximum Precipitation (PMP) Study for the Wanahoo Drainage Basin, Prepared for Olsson Associates, Omaha, Nebraska.

- Tomlinson, E.M., Kappel W.D., Parzybok, T.W., Hultstrand, D., Muhlestein, G., and B. Rappolt, June 2008: Site-Specific Probable Maximum Precipitation (PMP) Study for the Blenheim Gilboa Drainage Basin, Prepared for New York Power Authority, White Plains, NY.
- Tomlinson, E.M., Kappel W.D., and T.W. Parzybok, February 2008: Site-Specific Probable Maximum Precipitation (PMP) Study for the Magma FRS Drainage Basin, Prepared for AMEC, Tucson, Arizona.
- Tomlinson, E.M., Kappel W.D., Parzybok, T.W., Hultstrand, D., Muhlestein, G., and P. Sutter, December 2008: Statewide Probable Maximum Precipitation (PMP) Study for the state of Nebraska, Prepared for Nebraska Dam Safety, Omaha, Nebraska.
- Tomlinson, E.M., Kappel, W.D., and Tye W. Parzybok, July 2009: Site-Specific Probable Maximum Precipitation (PMP) Study for the Scoggins Dam Drainage Basin, Oregon.
- Tomlinson, E.M., Kappel, W.D., and Tye W. Parzybok, February 2009: Site-Specific Probable Maximum Precipitation (PMP) Study for the Tuxedo Lake Drainage Basin, New York.
- Tomlinson, E.M., Kappel, W.D., and Tye W. Parzybok, February 2010: Site-Specific Probable Maximum Precipitation (PMP) Study for the Magma FRS Drainage Basin, Arizona.
- Tomlinson, E.M., Kappel W.D., Parzybok, T.W., Hultstrand, D.M., Muhlestein, G.A., March 2011: Site-Specific Probable Maximum Precipitation Study for the Tarrant Regional Water District, Prepared for Tarrant Regional Water District, Fort Worth, Texas.
- Tomlinson, E.M., Kappel, W.D., Hultstrand, D.M., Muhlestein, G.A., and T. W. Parzybok, November 2011: Site-Specific Probable Maximum Precipitation (PMP) Study for the Lewis River basin, Washington State.
- Tomlinson, E.M., Kappel, W.D., Hultstrand, D.M., Muhlestein, G.A., and T. W. Parzybok, December 2011: Site-Specific Probable Maximum Precipitation (PMP) Study for the Brassua Dam basin, Maine.
- U.S. Weather Bureau, 1946: Manual for Depth-Area-Duration analysis of storm precipitation. *Cooperative Studies Technical Paper No. 1*, U.S. Department of Commerce, Weather Bureau, Washington, D.C., 73pp.



SUSITNA-WATANA HYDRO

Clean, reliable energy for the next 100 years.

**ALASKA ENERGY AUTHORITY
AEA11-022
13-1402-REP-123114**

Appendix B

Intermediate Flood Routing Technical Memorandum

14-08-TM



SUSITNA-WATANA HYDRO

Clean, reliable energy for the next 100 years.

**Technical Memorandum
14-08-TM
v1.0**

Susitna-Watana Hydroelectric Project Intermediate Flood Routing

AEA11-022



Prepared for:
Alaska Energy Authority
813 West Northern Lights Blvd.
Anchorage, AK 99503

Prepared by:
MWH
1835 South Bragaw St., Suite 350
Anchorage, AK 99508

May 2014

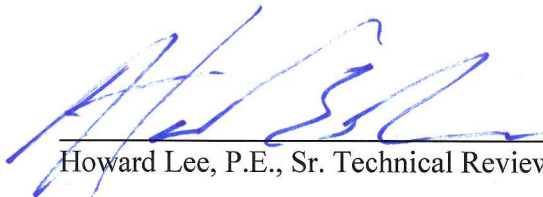
[This page intentionally blank.]

The following individuals have been directly responsible for the preparation, review and approval of this Technical Memorandum.

Prepared by: John Haapala, P.E., Senior Hydrologic/Hydraulic Engineer

Reviewed by: Julie Stanaszek, Senior Civil Engineer

Approved by:



Howard Lee, P.E., Sr. Technical Reviewer

Approved by:



Brian Sadden, Project Manager

Disclaimer

This document was prepared for the exclusive use of AEA and MWH as part of the engineering studies for the Susitna-Watana Hydroelectric Project, FERC Project No. 14241, and contains information from MWH which may be confidential or proprietary. Any unauthorized use of the information contained herein is strictly prohibited and MWH shall not be liable for any use outside the intended and approved purpose.

[This page intentionally blank.]



TABLE OF CONTENTS

1. INTRODUCTION..... 1

2. PEAK FLOW FREQUENCY 3

 2.1 Peak Annual Flows 3

 2.2 50-Year Annual Flood Peak..... 4

 2.3 50-Year Seasonal Flood Peak 5

3. FLOOD VOLUME FREQUENCY..... 8

 3.1 50-Year Annual Flood Volume..... 8

 3.2 50-Year July – September Flood Volume..... 8

4. 50-YEAR FLOOD INFLOW HYDROGRAPHS..... 10

 4.1 50-Year Annual Flood Hydrograph 10

 4.2 50-Year Seasonal Flood Hydrograph..... 11

5. RESULTS OF ALTERNATIVE ROUTINGS OF THE 50-YEAR FLOOD 12

 5.1 Diversion Flood Routing (During Construction) 12

 5.1.1 Diversion Facilities Description 12

 5.1.2 Diversion Flood Routing Results..... 12

 5.2 50-Year Surcharge Storage Flood Routings (During Operation) 13

 5.3 Comparison with 1980’s Results 17

6. BIBLIOGRAPHY 19



List of Tables

Table 1 Peak Annual Instantaneous Flows for the Susitna River at Gold Creek..... 3

Table 2 Calculated Flood Frequency for the Susitna River at Gold Creek 4

Table 3 Estimated Peak Annual Flows in the Susitna River at Watana Dam..... 5

Table 4 Reservoir Elevation – Capacity Data15

Table 5 Flood Routing Results16

Table 6 Summary of 1985 Flood Routing Study Results18

List of Figures

Figure 1 Reservoir Elevation Frequency..... 6

Figure 2 Watana Reservoir July – September Peak 1-Day Average Inflows 7

Figure 3 50-Year Annual Flood Hydrograph10

Figure 4 50-Year July - September Flood Hydrograph11

Figure 5 Run 6 Inflow, Outflow, and Reservoir Level17

List of Exhibits

Exhibit 1 Watana Reservoir Daily Inflows

1. INTRODUCTION

The primary purpose of this Technical Memorandum (TM) is to determine a range of potential operating scenarios for the 50-year flood (i.e. the 2% annual exceedance probability flood) from which a selected Project operation plan can be made with consideration of the tradeoffs in related factors. Factors that may be considered in the tradeoff evaluation include the low-level outlet works (LLOW) capacity versus the amount of reservoir storage used to attenuate the peak outflow during large flood events. Greater LLOW capacity would result in a smaller reservoir pool allocated to flood control storage and therefore a lower dam crest elevation. Increased LLOW capacity would result in a slight reduction in generation as less flood surcharge storage would be routed through the powerhouse. Downstream fluvial geomorphology and other environmental considerations may also factor into the flood surcharge operation. Also, the capability to pass a given discharge, such as the 2-year flood peak flow of 38,500 cfs indicated in Table 3 below, may be a factor in the selection of LLOW valve capacity.

A Probable Maximum Flood (PMF) study is being performed for the Susitna-Watana Hydroelectric Project (Project) by MWH under NTP 13. The PMF is the spillway design flood for Watana Dam, and as such the inflow PMF routed through the reservoir will ultimately determine the required capacity of the spillway, the total outflow capability at Watana Dam, the reservoir surcharge storage between the maximum normal pool level and the maximum flood pool level, and the final dam crest level that assures the flood safety of the dam.

To limit the frequency of spillway operation, which may result in undesirable downstream gas supersaturation, an operating criterion is being adopted such that the Project should be able to pass floods up to the 50-year flood without opening the spillway gates. Facilities that will be used to pass the 50-year flood include the powerhouse turbines and the fixed-cone valves in the LLOW as well as surcharge storage in the reservoir above the maximum normal operating level at El 2050. Floods larger than the 50-year flood ranging up to the PMF would require usage of the main spillway in addition to the LLOW.

The 50-year construction diversion flood was also routed with a limiting maximum reservoir level at El 1553, which is planned to be the top elevation of the impervious core of the upstream cofferdam.



SUSITNA-WATANA HYDRO

Clean, reliable energy for the next 100 years.

ALASKA ENERGY AUTHORITY

AEA11-022

13-1408-TM-022814

Results of the 50-year construction diversion flood routing provided herein will show whether there is any significant attenuation of the flood due to storage behind the cofferdam.

2. PEAK FLOW FREQUENCY

2.1 Peak Annual Flows

The most frequently referenced parameter for a rare flow event such as the 50-year flood is the peak flow. Peak annual flows in the Susitna River near the Project site have been recorded by the USGS at Gold Creek, as summarized in Table 1. Peak flow rates provided by the USGS include both average daily values and instantaneous peaks.

Peak flows for return periods up to 10,000 years were estimated for the Susitna River at Gold Creek. Peak flows were estimated for various return periods by fitting recorded peak flow data with a Log Pearson Type III distribution according to methods in Bulletin 17B (IACWD, 1982). Estimated peak annual flows for the Susitna River at Gold Creek are presented in Table 2.

Table 1 Peak Annual Instantaneous Flows for the Susitna River at Gold Creek

Date	Peak Flow (cfs)	Date	Peak Flow (cfs)	Date	Peak Flow (cfs)
June 21, 1950	34,000	June 30, 1970	33,400	September 15, 1990	50,300
June 8, 1951	37,400	August 10, 1971	87,400	June 23, 1991	35,300
June 17, 1952	44,700	June 17, 1972	82,600	July 19, 1992	33,300
June 7, 1953	38,400	June 16, 1973	54,100	September 3, 1993	36,300
August 4, 1954	42,400	May 29, 1974	37,200	June 22, 1994	46,600
August 26, 1955	58,100	June 3, 1975	47,300	June 25, 1995	37,800
June 9, 1956	51,700	June 12, 1976	35,700	August 26, 1996	26,100
June 8, 1957	42,200	June 15, 1977	54,300	August 1, 2001	40,200
August 3, 1958	49,600	June 23, 1978	25,000	August 23, 2002	36,200
August 25, 1959	62,300	July 16, 1979	41,300	July 28, 2003	51,700
September 13, 1960	41,900	July 29, 1980	51,900	May 8, 2004	43,400
June 23, 1961	54,000	July 12, 1981	64,900	June 19, 2005	50,200
June 15, 1962	80,600	June 21, 1982	37,900	August 20, 2006	59,800
July 18, 1963	49,000	June 3, 1983	37,300	May 28, 2007	30,800
June 7, 1964	90,700	June 17, 1984	59,100	July 30, 2008	34,400
June 28, 1965	43,600	May 28, 1985	40,400	May 5, 2009	40,400
June 6, 1966	63,600	June 18, 1986	29,100	July 22, 2010	37,400
August 15, 1967	80,200	July 31, 1987	47,300	May 29, 2011	46,300
May 22, 1968	41,800	June 16, 1988	43,600	September 21, 2012	72,000
May 25, 1969	28,400	June 15, 1989	46,800	June 1, 2013	90,500

Table 2 Calculated Flood Frequency for the Susitna River at Gold Creek

Return Period (Years)	Flow (cfs)
2	44,700
5	58,600
10	68,700
25	82,700
50	93,800
100	106,000
200	118,000
500	135,000
1,000	149,000
10,000	195,000

2.2 50-Year Annual Flood Peak

Peak flows were estimated for return periods up to 1,000 years at the Watana Dam site by transposing peak flow analysis results at Gold Creek to Watana according to the following equation:

$$Q_{Watana} = Q_{Gold\ Creek} \times \left(\frac{A_{Watana}}{A_{Gold\ Creek}} \right)^{0.86}$$

where A is the drainage area for each site. Peak flows are frequently adjusted from a gaged to an ungaged location by the ratio of the square root of the drainage areas. A USGS publication on the Flood Characteristics of Alaskan Streams (Water Resources Investigations 78-129), indicates that the exponent of the drainage area ratio should be at about the selected 0.86 value. The annual flood frequency values for Watana Dam presented in Table 3 can also be used to develop the construction diversion floods. The resulting 50-year annual instantaneous flood peak is 80,800 cfs.

Table 3 Estimated Peak Annual Flows in the Susitna River at Watana Dam

Return Period (Years)	Flow (cfs)
2	38,500
5	50,500
10	59,200
20	68,300
25	71,300
50	80,800
100	91,300
500	116,300
1,000	128,400

2.3 50-Year Seasonal Flood Peak

The initial reservoir elevation at the beginning of a flood is an important parameter for flood routing modeling. If the reservoir elevation was below El 2050 at the start of the 50-year flood, much or all of the 50-year flood water would fill the reservoir up to El 2050, the point at which surcharge storage operations would begin and results would indicate a reduced need for fixed-cone outlet valve discharge capacity. The months when the reservoir elevation is very unlikely to be at El 2050 are therefore eliminated from the analysis so that the assumed initial reservoir elevation can be set at El 2050.

As is standard procedure at the feasibility level of studies, a number of preliminary reservoir operation cases have been tested. Figure 1 is a reservoir elevation frequency diagram, derived from the current power operation modeling preliminary Run 11C. Only the months of May through September need to be considered for the 50-year annual flood because these are the only months of occurrence of the peak annual flood in 134 station-years of record at the Susitna River USGS gaging stations at or above Gold Creek where the Project is located. For the 50-year seasonal flood, May is eliminated because the reservoir is never full (i.e. at El 2050) during May. June can also be eliminated because the reservoir is full less than 1% of the time in June, which means that the maximum June reservoir levels are the end result of a sequence of high inflows, not the initial level, so large floods after that month are very unlikely. For routing of a 50-year flood, a June full reservoir (El 2050) starting elevation would be an excessively conservative assumption.

The remaining months when historical annual peak flows have been observed to occur and when the reservoir is more likely to be full are July, August, and September. Therefore, a seasonal flood frequency analysis was performed for the months of July through September to develop the seasonal 50-year flood for detailed flood routing through the surcharge storage pool above El 2050. This same seasonal duration was used in the 1985 Susitna study.

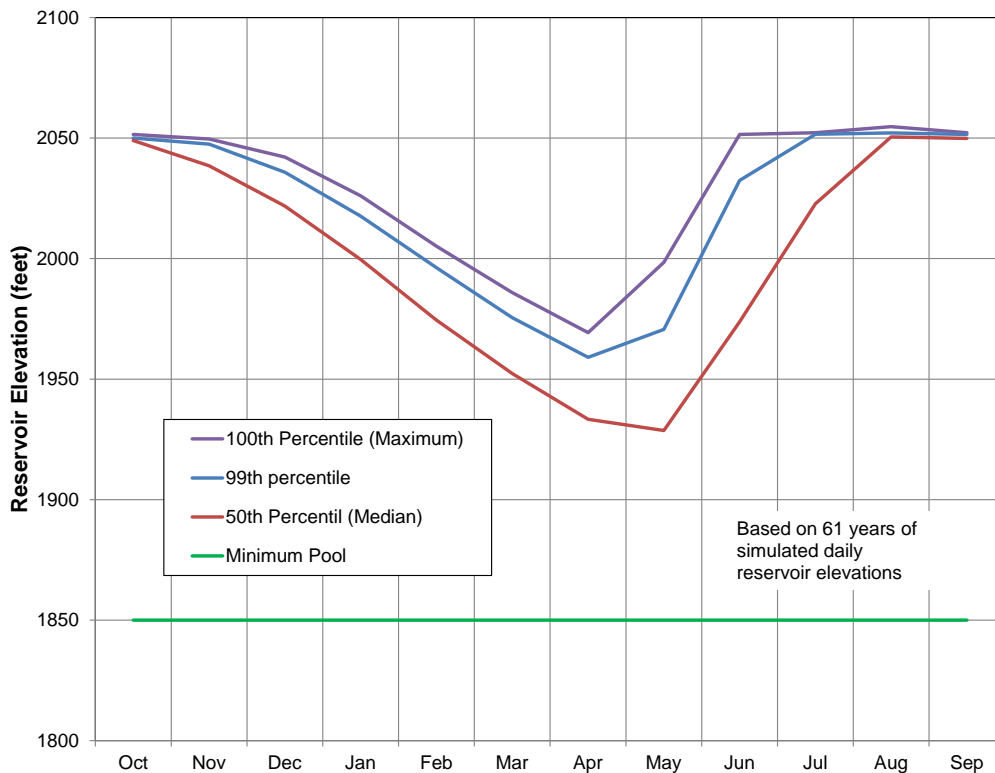


Figure 1 Reservoir Elevation Frequency

The basic source of seasonal flow data was the 61 years of daily Watana Reservoir inflows as developed from the USGS record extension study for the Susitna River basin (Curran 2012). For reference, the 61 years of daily inflows to Watana Reservoir are plotted on the attached Exhibit 1. A frequency analysis of the annual 1-day maximum Watana Reservoir inflow in the July through September period is shown on Figure 2. The 50-year 1-day inflow from the frequency analysis is 57,900 cfs. The largest 1-day inflow as developed from the historic record was 66,800 cfs in August 1971, which was also the largest month of August inflow. The second largest 1-day inflow was 60,800 cfs in August 1967, which was also the third highest month of August inflow to the reservoir.

An analysis of the five largest August through September recorded peak flows at the USGS gage at Gold Creek showed that peak instantaneous flows were 5% to 12% larger than the average daily flows, with the average value being 8% larger. The calculated 50-year 1-day average flow of 57,900 cfs would equate to an instantaneous peak flow of 62,500 cfs with the average 8% increase.

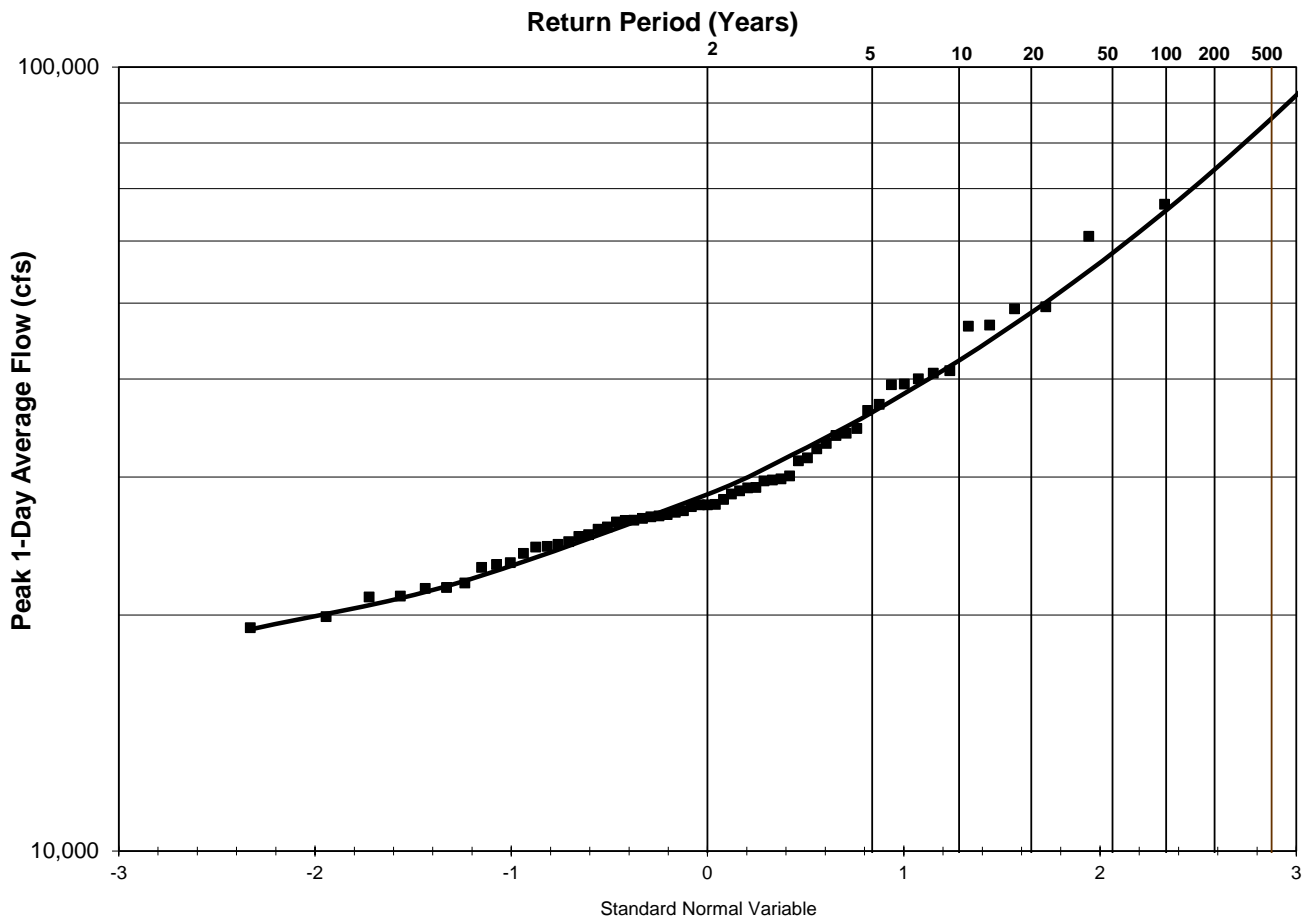


Figure 2 Watana Reservoir July – September Peak 1-Day Average Inflows

For reference, the September 2012 flood had a peak daily flow of 58,700 cfs and an instantaneous peak of 60,700 cfs at the USGS gaging station at Tsusena Creek, which has a drainage area essentially the same as Watana Dam. The September 2012 flood was by far the largest September flood of record at the USGS gaging station at Gold Creek.

3. FLOOD VOLUME FREQUENCY

The 50-year floods were routed through the reservoir to determine the peak water levels and peak outflows. During construction, the diversion flood would start at about El 1465, near the bottom of an unfilled reservoir wherein the area is relatively small. The storage space available for inflow flood attenuation would be small, about 29,000 acre-feet up to the elevation 1553, the top of the impervious core of the diversion cofferdam. During operation, the 50-year July–September flood would begin at El 2050, the maximum normal pool level, which means that storage space available for inflow flood attenuation is much greater.

As a conservative design parameter, the 50-year flood hydrographs to be routed through the reservoir were developed to contain not only the 50-year peak inflow, but also the 50-year total hydrograph volume. A review of historic hydrographs indicates that the high flows of maximum floods tend to occur over a period of about 20 days. Therefore, the 50-year flood should embody the 50-year, 20-day volume as well as the 50-year flood peak. In a manner similar to the determination of the 50-year 1-day average floods at Watana Dam, the 50-year 20-day average flood flow was determined.

3.1 50-Year Annual Flood Volume

A statistical analysis of the 61-year Watana Dam inflow record indicates that the all-season 50-year 20-day average inflow volume would be 39,900 cfs (1,583,000 acre-feet total over 20 days). In the developed 61-year period of Watana inflow record, the maximum 20-day average volume was 50,210 cfs (1,992,000 acre-feet total over 20 days) in June 1964. The second maximum 20-day average in the 61-year period of record was 40,670 cfs (1,613,000 acre-feet total over 20 days) in June 1962 and the third largest in 61 years was an average of 33,800 cfs (1,341,000 acre-feet total over 20 days) in August 1981. By comparison to those three historical maximum values, the calculated volume of 1,583,000 acre-ft over 20 days was confirmed for the 50-year annual flood volume.

3.2 50-Year July – September Flood Volume

For the July through September season, the calculated 50-year 20-day average Watana inflow volume was 34,100 cfs (1,353,000 acre-feet total over 20 days). The two largest 20-day average flows in the



SUSITNA-WATANA HYDRO

Clean, reliable energy for the next 100 years.

ALASKA ENERGY AUTHORITY

AEA11-022

13-1408-TM-022814

61-year period of estimated inflow record were 33,800 cfs (August 1981), and 32,900 cfs (September 1959). Because of the clustering of maximum values, the 50-year 20-day volume of 1,353,000 acre-feet was considered to be acceptable.

4. 50-YEAR FLOOD INFLOW HYDROGRAPHS

The shape of the 50-year inflow hydrographs was based on historic floods for the appropriate season as taken from the calculated 61-year period of Watana Reservoir daily inflows. Historic floods that had a single peak and a classic hydrograph shape were favored. The historic hydrographs were scaled to provide the desired peak flow and volume with some rearranging of flows to give ascending flows before the peak and descending flows after the peak of the hydrograph.

4.1 50-Year Annual Flood Hydrograph

The 50-year annual flood hydrograph shape was based on the June 1971 flood for which the historic inflow at Watana was estimated to be 66,800 cfs with a 20-day volume of 1,285,000 acre-feet. The rescaled 50-year annual peak flow was 80,800 cfs and the 20-day volume was 1,581,000 acre-feet. The 50-year annual flood is plotted on Figure 3.

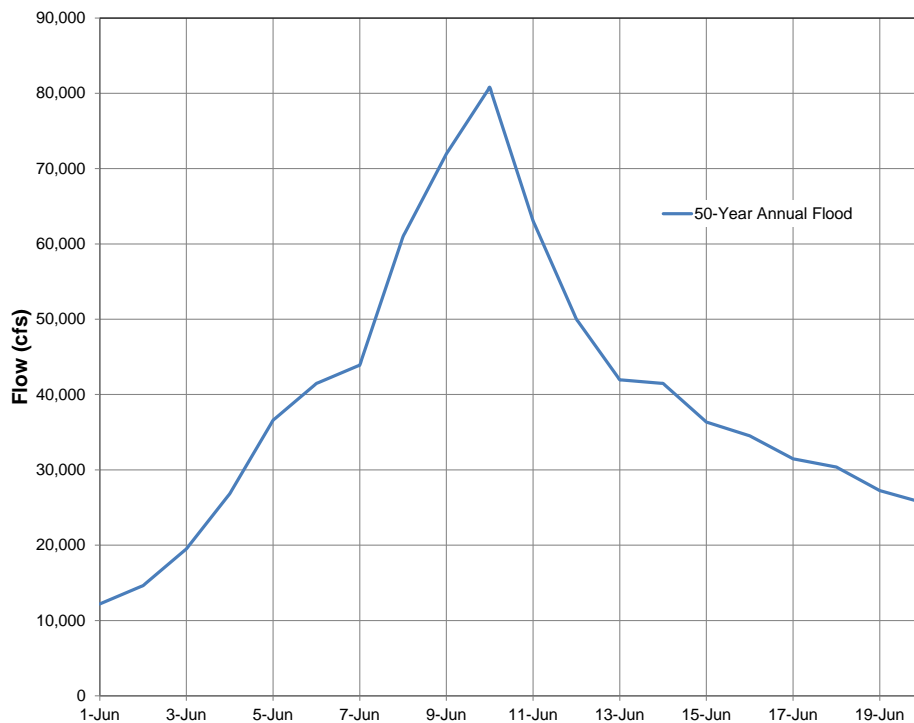


Figure 3 50-Year Annual Flood Hydrograph

4.2 50-Year Seasonal Flood Hydrograph

The 50-year July-September seasonal flood was based on the August 1971 historical flood for which the peak daily flow at Watana was 66,800 cfs and the 20-day volume was 1,265,000 acre-feet. The peak flow for the 50-year seasonal flood, as shown on Figure 4, is 62,500 cfs and the 20-day volume is 1,352,000 acre-feet.

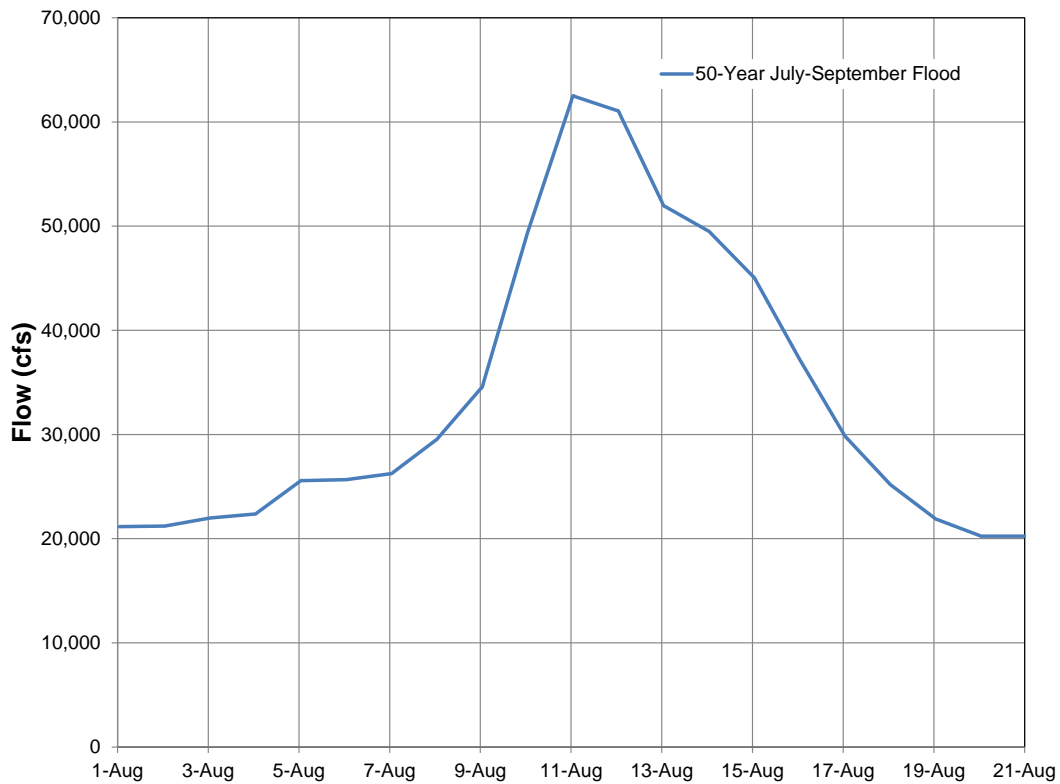


Figure 4 50-Year July - September Flood Hydrograph

5. RESULTS OF ALTERNATIVE ROUTINGS OF THE 50-YEAR FLOOD

The HEC-1 Flood Hydrograph Package was used for routing the floods through the available reservoir storage. Daily inflows were input to the model, which disaggregated the daily data to hourly data, as plotted on Figure 3 and Figure 4.

5.1 Diversion Flood Routing (During Construction)

5.1.1 Diversion Facilities Description

The construction diversion facilities would consist of the following main components:

- An upstream cofferdam with crest at El 1560 and an impervious core at El 1553. The upstream cofferdam would have a 120-ft wide overflow spillway on each abutment with a crest level at El 1530.
- A 36-ft diameter, vertical sided, horseshoe-shaped, lined diversion tunnel. The enlarged tunnel entrance would have two 22-ft wide by 36-ft high gated intakes. The design criterion is that the tunnel alone should pass the 5-year flood assuming no hydraulic capacity reductions due to ice or debris.
- A 44-ft wide (50-ft wide at the entrance) by 44-ft high sluice through the RCC main dam. The design criterion is that the sluice alone should pass the 50-year flood under the conservative assumption that the tunnel is completely plugged.
- A downstream cofferdam designed to wash away in the event that the sluice operates.

5.1.2 Diversion Flood Routing Results

Results of the diversion flood routings indicate that the available storage upstream of the cofferdam is insufficient to attenuate the 80,800 cfs peak of the 50-year annual inflow flood shown in Figure 3 in any meaningful way such that the diversion facilities essentially must pass the entire peak of the inflow flood. The storage impounded by the cofferdam up to the top of the impervious core at El 1553 is only

about 29,000 acre-feet. An inflow of 50,000 cfs, which occurs for several days during the 50-year flood, would have a daily inflow volume of about 100,000 acre-feet.

Because the potential for at least partial plugging of the diversion tunnel with ice floes cannot be dismissed, the following two cases were run:

- The first case assumes no hydraulic capacity reductions of the diversion tunnel and includes usage of the sluice. The calculated peak outflow was 80,050 cfs at a peak reservoir level at elevation 1540.4.
- The second case assumes the most extreme case of complete plugging of the diversion tunnel. The calculated peak outflow was 80,090 cfs at a peak reservoir level at elevation 1552.6.

5.2 50-Year Surcharge Storage Flood Routings (During Operation)

As used herein, 50-year surcharge storage means the reservoir storage between the maximum normal pool level at El 2050 and the maximum water level of the 50-year routed seasonal flood. An additional increment of reservoir storage may be used for routing of the Probable Maximum Flood (PMF). The objective of the surcharge storage flood routings is to provide enough information so that an informed choice of fixed-cone outlet valve capacity and surcharge storage can be made.

Assumptions and analysis parameters that are constant or are can vary between runs include the following:

- The initial reservoir level is at El 2050 in all runs.
- The 50-year seasonal (July – September) flood is the inflow flood.
- The gated spillway is not to be used because spillway flows could potentially cause gas supersaturation downstream from Watana Dam.
- The emergency (diversion tunnel) outlet is not to be used.
- Flood forecasting is not used to improve the surcharge storage operation.

- The number and total capacity of the fixed-cone outlet valves is a variable. Each fixed-cone valve is assumed to have a capacity of 4,000 cfs.
- The fixed-cone valves begin to open as soon as the reservoir level rises above El 2050.
- The reservoir level at which the fixed-cone valves are fully open is a variable.
- The amount of turbine flow up to the 15,000 cfs capacity is a variable. The turbine flows are assumed to be constant during the flood routing.

The primary results of the analysis are peak reservoir level and peak total outflow.

Both pluses and minuses can be assigned to the variables. Increased fixed-cone valve capacity and a faster rate of opening of the valves would reduce the amount of necessary surcharge storage and thus reduce the height and cost of the dam. But flow through the fixed-cone valves is essentially “spill”, released water that is not available for generation, so there is a resulting power loss which is a disincentive to use them. Fluvial geomorphology considerations tend to favor releasing higher flows that are capable of moving sediment and maintaining natural channel characteristics.

Assuming an operating rule for the fixed-cone valves where the valves would hold the reservoir level at exactly El 2050 could result in a very abrupt opening of the valves. The reservoir could store the early part of the flood hydrograph but El 2050 could be reached at a high flow, say 50,000 cfs, that could require immediate maximum valve flows. Forecasting of inflows could be done to improve the operation, such as beginning to open the valves more gradually before El 2050 is reached, but no prior knowledge of inflow rates is assumed herein for the present analysis.

For routing of the PMF, the normal assumption is that the turbines are not operating due to extremely stormy conditions and associated power outages or transmission line drops. This is not necessarily the case for routing of a much smaller flood such as the 50-year flood, so the turbines are assumed to be operable for that case. The areas of greatest energy consumption are far from Watana Dam and may not be experiencing unusually stormy conditions. The July through September time period is not the period of peak power demand, so maximum power output at Watana may not be usable and energy production

may be limited. Therefore, it may not be reasonable to assume the powerhouse could discharge at maximum output, which would correspond to a maximum flow of about 15,000 cfs. Releases above those made through the powerhouse would need to be made through the LLOW.

The expected PMF operation will be for the turbines to operate until the maximum 50-year flood reservoir elevation is achieved and then the turbines will shut down and the spillway gates will begin to open. Because the fixed-cone valves are assumed to be operational for both the 50-year flood and the PMF, incorporation of additional fixed-cone valves could result in a corresponding reduction in required spillway capacity. This is a tradeoff that is being evaluated as part of the ongoing engineering feasibility studies.

The 1980s Susitna feasibility study allocated 14 feet of reservoir flood storage space above the maximum normal pool level before the spillway gates began to open. In the current feasibility studies it was anticipated that the current design would use at least a few feet of reservoir storage to attenuate the inflow flood, rather than passing the entire peak of the inflow flood without an increase in reservoir level. Table 4 provides the reservoir elevation-volume table for the elevation range of potential flood surcharge storage.

Table 4 Reservoir Elevation – Capacity Data

Elevation (feet)	Reservoir Volume (acre-feet)
2050	5,170,000
2055	5,289,300
2060	5,407,900
2065	5,530,900
2070	5,654,500
2075	5,780,400

A range of flood routings were performed using the HEC-1 model; results are summarized in Table 5. The range of possible fixed-cone valve capacity covered was from 24,000 cfs (6 valves operating) to 40,000 cfs (10 valves operating) in combination with the turbines discharging at about full or half capacity. Also tested in the modeling was a slower opening of the valves that would be done to save

some additional water for generation, which showed that raising the full-open level of the valves by 1-foot results in a corresponding 1-foot increase in the peak reservoir level. The results of the model runs shown in Table 5 are available for evaluation and selection of the preferred configuration by AEA.

Table 5 Flood Routing Results

Run	All Turbines Maximum Total Outflow (cfs)	Valves Maximum Total Outflow (cfs)	All Valves Fully Open Elevation (feet)	Peak Outflow (cfs)	Peak Reservoir Elevation (feet)	Comments
1	15,000	24,000	2051	39,000	2057.9	Similar in concept to 1980s design
2	7,500	24,000	2051	31,500	2062.4	Reduces turbine output due to lower load
3	15,000	28,000	2051	43,000	2055.8	Like Run 1, but adds 1 valve
4	7,500	28,000	2051	35,500	2059.9	Like Run 2, but adds 1 valve
5	15,000	32,000	2051	47,000	2054.1	Like Run 1, but adds 2 valves
6	7,500	32,000	2051	39,500	2057.6	Like Run 2, but adds 2 valves
7	15,000	36,000	2051	51,000	2052.8	Like Run 1, but adds 3 valves
8	7,500	36,000	2051	43,500	2055.6	Like Run 2, but adds 3 valves
9	15,000	40,000	2051	55,000	2051.9	Like Run 1, but adds 4 valves
10	7,500	40,000	2051	47,500	2053.9	Like Run 2, but adds 4 valves
11	15,000	36,000	2052	51,000	2053.8	Like Run 7, but opens valves more slowly
12	7,500	36,000	2052	43,500	2056.6	Like Run 8, but opens valves more slowly

Figure 5 is an example plot of the flood routing for Run 6. The reservoir level is output by HEC-1 in 0.1 ft increments that results in a slightly jagged plot of reservoir elevation. As shown, the peak elevation rise for the reservoir is 7.6 feet (El 2050.0 to El 2057.6), and that peak occurs about 15 days after the flood begins.

AEA has evaluated the results presented in Table 5, and Run 6 was the selected alternative. Therefore, the proposed Watana Dam configuration will include 8 fixed-cone valves, each capable of discharging 4,000 cfs with the reservoir level at El 2050 for a maximum fixed-cone valve outlet capability of 32,000 cfs. For routing of the PMF, the following conditions will be incorporated:

- The 8 fixed-cone valves will begin to open when the reservoir level rises above El 2050.0 and will become fully open when the reservoir level reaches El 2051.0.
- Turbine flow will be 7,500 cfs until the reservoir reaches El 2057.6, at which point the turbines will be completely shut down for the remainder of the PMF routing.

- The spillway gates will not begin to open until the reservoir level has reached El 2057.6.
- The size of the spillway gates and the total outflow capability of the spillway will be as determined in the PMF Study.

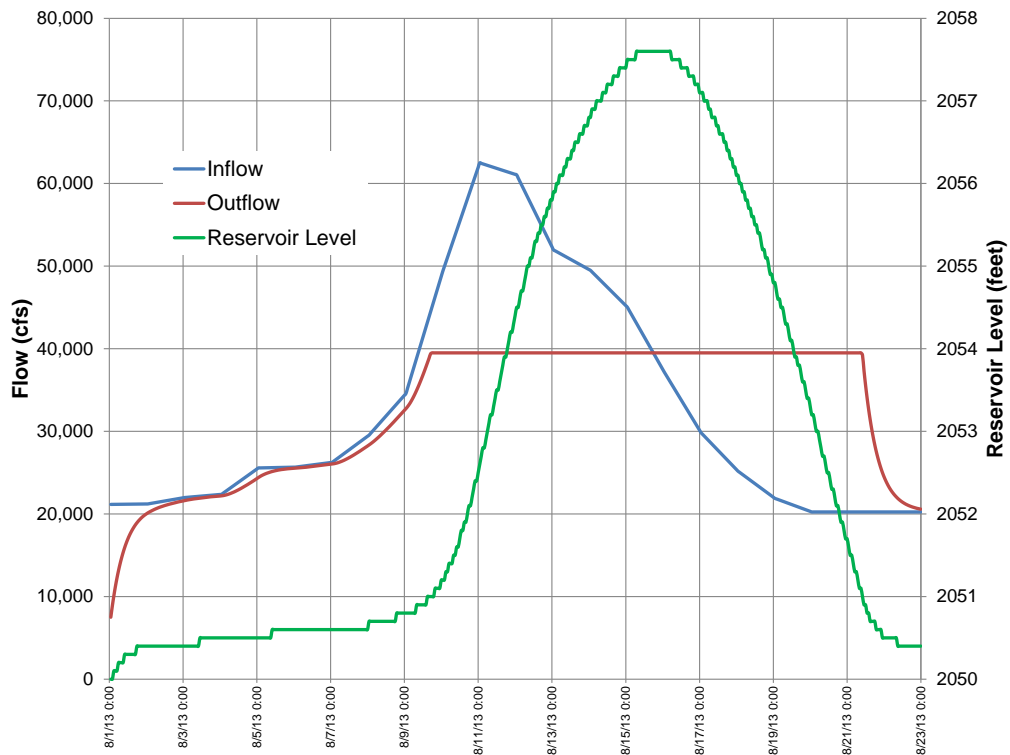


Figure 5 Run 6 Inflow, Outflow, and Reservoir Level

5.3 Comparison with 1980's Results

For comparison, results from the 1985 FERC License Application for the Susitna Project are shown in Table 6. Based on plots of the study results, it appears that the spillway gates began to open at a level higher than the peak of the 50-year July – September flood. The reasons for this difference have not been evaluated to date.

Table 6 Summary of 1985 Flood Routing Study Results

Parameter	1985 Watana Stage I	1985 Watana Stage III
Maximum normal pool level (feet)	2000.0	2185.0
Fixed-cone valves total capacity (cfs)	24,000	30,000
50-year flood peak reservoir level (feet)	2011.0	2191.5
50-year flood peak outflow (cfs)	34,000	33,900
Elevation that spillway begins to operate (feet)	2014.0	2193.0
PMF peak reservoir level (feet)	2017.1	2199.3
PMF peak outflow (cfs)	302,000	284,000

6. BIBLIOGRAPHY

1. Alaska Power Authority, November 1985. *Supporting Design Report*, Susitna Hydroelectric Project, Draft License Application, Volume 16, Exhibit F.
2. Curran, J.H., 2012. *Streamflow Record Extension for Selected Streams in the Susitna River Basin*, Alaska, U.S. Geological Survey Scientific Investigations Report 2012-5210, 36 p.
3. MWH, 2014. *Interim Feasibility Report*, Susitna-Watana Hydroelectric Project.
4. MWH, 2014. *Probable Maximum Flood Study*, Susitna-Watana Hydroelectric Project.



Exhibit 1

Watana Reservoir Daily Inflows

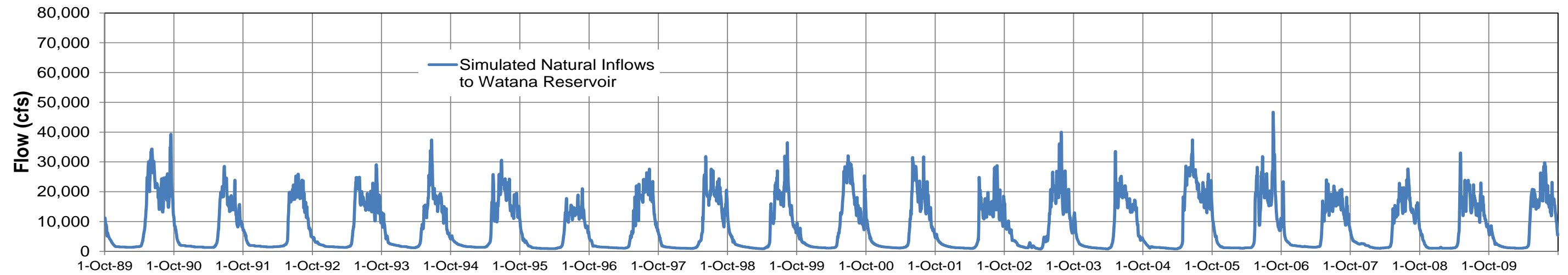
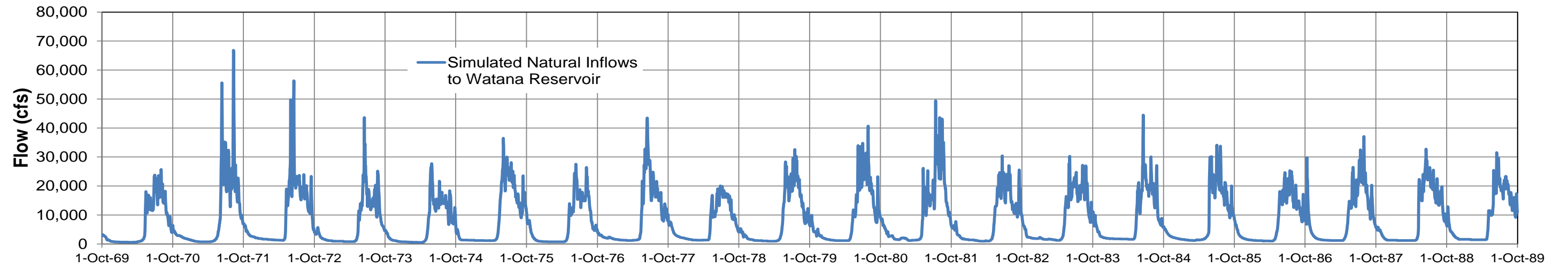
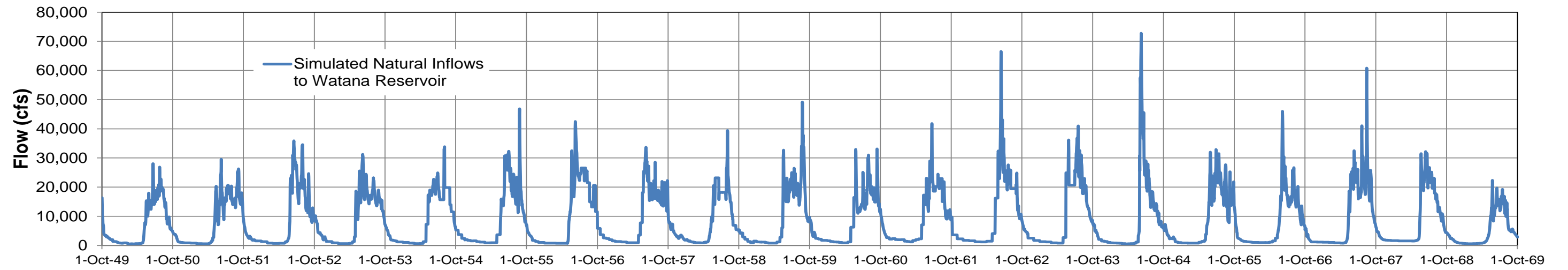


Exhibit 1: Watana Reservoir Daily Inflows